Title
Transportation Modeling For The Environment

Authors
Barth, Matthew J.
Norbeck, Joseph M.

Publication Date
1994

CALIFORNIA PATH PROGRAM
INSTITUTE OF TRANSPORTATION STUDIES
UNIVERSITY OF CALIFORNIA, BERKELEY

Transportation Modeling for the Environment

Matthew J. Barth
Joseph M. Norbeck
University of California, Riverside

California PATH Research Report
UCB-ITS-PRR-94-27

This work was performed as part of the California PATH Program of the University of California, in cooperation with the State of California Business, Transportation, and Housing Agency, Department of Transportation; and the United States Department of Transportation, Federal Highway Administration.

Report for MOU 105

December 1994

ISSN 1055-1425

Preface

This interim research report has been prepared for the California PATH Program, MOU #105, entitled “Transportation Modeling for the Environment”. This report covers the work that has been performed in the first year of a two year research project. Contributions to this report have been made by Joseph Norbeck, Ramakrishna Tadi, Rosa Fitzgerald, Robert Frankle, Gary Zheng, and Eric Johnston. Comments made by the reviewers of the original draft document were very useful. It is also important to acknowledge David Chock and James Butler from Ford Motor Company, who have provided considerable data and information on vehicle emissions. Parts of this report have been taken from other research reports written at the Center for Environmental Research and Technology.

Abstract

Transportation Modeling for the Environment

Matthew J. Barth and Joseph M. Norbeck

College of Engineering
Center for Environmental Research and Technology
University of California, Riverside, CA 92521

May, 1994

Intelligent Transportation Systems (ITS) offer the potential to improve highway safety, reduce highway congestion, and increase economic productivity. However, it is not clear what the effect ITS will have on air quality, specifically, vehicle emissions. As a result of various ITS technological bundles, average vehicle emissions should decrease due to smoother traffic flow and less congestion. In contrast, the transportation system may become more attractive, inducing greater travel demand and higher VMT (vehicle-miles traveled), resulting in an increase of emissions. In this research report, we describe preliminary research dealing with vehicle emissions associated directly with 1) Automated Highway Systems (AHS) and 2) ramp metering. In performing this analysis, a power-demand modal emissions model has been integrated with several transportation simulation models in order to quantitatively determine the effects of ITS technology on vehicle emissions. For AHS, a steady-state speed/emissions comparison has been conducted between vehicles that are platooned and non-platooned. Due to the reduction of aerodynamic drag while platooning (the "drafting" effect), the emissions for the platoon are significantly lower at higher steady-state speeds. Further, a comparison has been made between a platoon under optimized and non-optimized CICC (Coordinated Intelligent Cruise Control) and AICC (Autonomous Intelligent Cruise Control) control laws. For ramp metering, an initial evaluation has been conducted concentrating on the effect of vehicle emissions. Three components of ramp metering were evaluated independently: 1) the effect of freeway traffic smoothing; 2) ramp and surface street congestion; and 3) hard accelerations from the ramp meters.

KEY WORDS: environmental impacts, emissions, transportation simulation modeling, Automated Highway Systems (AHS), platooning, ramp metering

Executive Summary

Intelligent Transportation Systems (ITS, formerly IVHS) have generated considerable enthusiasm in the transportation community as potential methods to improve highway safety, reduce highway congestion, enhance the mobility of people and goods, and to promote the economic productivity in the country's transportation system. However, it is uncertain what effect ITS will have on air quality, specifically, vehicle emissions. There are primarily two influential factors: 1) Potentially, vehicle emissions can be reduced through the implementation of several ITS technological bundles. Advanced Vehicle Control Systems (AVCS) implemented at the vehicle level will safely smooth the traffic flow, minimizing the stop-and-go effect that leads to higher emissions. Advanced Traffic Management/Information Systems (ATMIS) will minimize congestion and subsequently emissions, for example by allowing dynamic re-routing to take place on the roadway network, and aiding in trip-chaining practices. 2) In contrast, the implementation of ITS technologies may induce traffic demand that leads to an increase of total vehicle miles traveled (VMT) by making the transportation system more desirable. For example, if ITS allows smoother flow and higher speeds on the roadways, people may choose to live farther away from work while still commuting in the same amount of time. In this research, we have begun to evaluate the direct impact of ITS traffic operation on vehicle emissions. We concentrate on the actual implementations of proposed strategies, and do not consider the effect of potential induced traffic demand as outlined above.

In order to determine the direct impact of ITS technologies on air quality, significant improvements must be made in traffic simulation and travel demand models by closely integrating vehicle emission models. Existing traffic, emissions, and planning models have been developed independently of each other and are difficult to integrate together when determining accurate air quality impacts. Current emission models (i.e., MOBILE, developed by the US Environmental Protection Agency (EPA) and EMFAC, developed by the California Air Resources Board (CARB)) functionally relate emissions to average vehicle speed and density, and are not appropriate for analyzing ITS scenarios. Under ITS conditions, the dynamic behavior of vehicles will be very different compared to today's traffic conditions, upon which the current emissions models are based. As a result, *modal emissions data* (i.e., emissions data associated with vehicle modes, e.g., idle, acceleration, cruise, deceleration, etc.) can be used with microscale traffic simulations to obtain more realistic results.

We have begun to integrate a power-demand modal emissions model with several simulation models in order to quantitatively determine the effects of ITS technology on vehicle emissions.

The vehicle dynamics equations and load-based emissions used in this study have been calibrated to a modern, closed-loop emission controlled vehicle (1991 Ford Taurus). As further modal emission data becomes available for other vehicles, they can easily be incorporated into the models when determining a more complete, comprehensive emissions estimate. Even though the preliminary results in this report are based on a single vehicle, trends are seen and important conclusions can be made regarding the importance of linking modal emissions with dynamic vehicle activity.

In the first year of work, we have enhanced previously developed transportation/emission models to study: 1) vehicle platooning that will take place within an Automated Highway System (AHS), and 2) ramp metering used to smooth traffic flow on the freeways.

For AHS, a steady-state speed/emissions comparison has been conducted between vehicles that are platooned and non-platooned. Due to the reduction of aerodynamic drag while platooning (the "drafting" effect), the emissions for the platoon are significantly lower at higher steady-state speeds. Preliminary results indicate that with AHS's approximate four-fold increase of capacity, emissions will increase over current manual conditions by a factor of two if the system is used at full capacity (~8000 vehicles/hour-lane), stay the same at half capacity (~4000 vehicles/hour-lane), and will decrease by half at current traffic volumes (~2000 vehicles/hour-lane). Further, a comparison has been made between a platoon under optimized and non-optimized CICC (Coordinated Intelligent Cruise Control) control laws. In the optimized case, control constants are set at their optimized values for best maintaining intraplatoon spacing. For the non-optimized case, these control constants are perturbed and the resulting emissions are compared to the optimized case. At high speeds under high load conditions, the non-optimized case tends to produce higher emissions. Finally, various driving cycles (velocity profiles of on-road vehicle motion) have been simulated for both CICC and AICC (Autonomous Intelligent Cruise Control) platoon operations. Although platoons will be operated smoothly in a typical AHS, more aggressive driving cycles were used in simulation in order to identify potential emission producing events. For specific velocity transients, hard accelerations and decelerations were often required of follower vehicles to maintain proper platoon formation. These accelerations often lead to short bursts of high emissions during the driving cycles, depending on the control laws governing intraplatoon spacing. A comparison of total emissions has been carried out using CICC and AICC control laws. The results indicate no significant difference in emissions produced.

For ramp metering, an initial evaluation has been conducted concentrating on the effect of vehicle emissions. Three components of ramp metering were evaluated independently: 1) the

effect of freeway traffic smoothing; 2) ramp and surface street congestion; and 3) hard accelerations from the ramp meters. Through the use of simulation, it has been shown that the mainline freeway average traffic speed decreases as the traffic volume of a freeway on-ramp increases. Further, if ramp metering is used, it has been shown that the mainline traffic speeds increase as a function of the ramp meter cycle time. Based on the assumptions and models used in this report, emissions for the mainline freeway tend to reach a maximum for a ramp meter cycle time near two seconds, but then fall as the cycle time increases. Similarly, total emissions associated with vehicles on the ramp waiting to enter the freeway decrease with an increase in ramp meter cycle times. Finally, emissions corresponding to hard accelerations from the meter to the freeway merge point can be significant if the required acceleration places a high power demand on the individual vehicle engines. A comparison was also made of the velocity and acceleration profiles from a ramp acceleration simulation model with profiles that were measured in the field. It was shown that the ramp acceleration model which assumed a constant power delivery from the engine generated velocity/acceleration profiles that do not match very well with actual velocity/accelerations measured in the field.

This preliminary evaluation of AHS and ATMIS strategies (such as ramp metering) on vehicle emissions will continue into the second year with a higher level of detail and further testing using more extensive data.

Table of Contents

1 Introduction……1

1.1 Emissions Modeling……2

1.2 Transportation Modeling ……5

1.3 Integrated Transportation/Emission Model Summary……7

1.4 Project Task Outline……8

1.4.1 Task 1: Transportation/Emissions Model Enhancement for ITS ……8

1.4.2 Task 2: Initial Study of AVCS Strategies …… 10

1.4.3 Task 3: Initial Study of ATMIS Strategies …… 10

2 Automated Highway System (AHS) Vehicle Emissions…… 13

2.1 Uninterrupted Traffic Flow…… 13

2.2 Platooning …… 15

2.3 Platoon Simulation Model…… 16

2.3.1 Vehicle Dynamics …… 17

2.3.2 Longitudinal Control…… 19

2.3.3 Platoon Generation …… 20

2.3.4 Simulation Flow …… 20

2.3.5 Graphical User Interface…… 22

2.4 Steady-State Velocity Emissions…… 22

2.5 Transient Velocity Emissions…… 28

2.5.1 Optimized vs. Non-Optimized CICC comparison …… 30

2.5.2 CICC vs. AICC comparison…… 34

3 Vehicle Emissions due to Ramp Metering …… 37

3.1 Mainline Traffic Smoothing…… 37

3.1.1 FRESIM Summary …… 39

3.1.2 Simulation Setup…… 39

3.1.3 Mainline Speed Reduction from High Ramp Volumes..... 40

3.1.4 Mainline Speed Increase from Ramp Metering 41

3.2 Ramp Queuing 43

3.3 Hard Ramp Accelerations 47

4 Conclusions and Future Work 53

4.1 AHS Vehicle Emissions 53

4.2 Ramp Meter Emissions 54

5 References 55

Appendix A.....A1

List of Tables and Figures

Figure 1.1. Current Emission Inventory Process 2

Figure 1.2. Hybrid macroscopic / microscopic modeling approach of ITEM 8

Figure 2.1. Flow, density, and speed relationship of uninterrupted traffic flow 14

Figure 2.2. Flow-density relationship for manual traffic 14

Figure 2.3. Platoons of vehicles on a highway 15

Figure 2.4. Traffic Flow-density relationship for manual and automated driving 16

Figure 2.5. Overall flowchart of platoon simulation 21

Figure 2.6. Graphical user interface of platoon simulation 23

Figure 2.7a. Velocity CO emission rates for 20 vehicles platooned and non-platooned 24

Figure 2.7b. Velocity HC emission rates for 20 vehicles platooned and non-platooned 24

Figure 2.7c. Velocity NOx emission rates for 20 vehicles platooned and non-platooned 25

Figure 2.8a. Total CO emissions versus traffic flow for manual and automated traffic 26

Figure 2.8b. Total HC emissions versus traffic flow for manual and automated traffic 27

Figure 2.8c. Total NOx emissions versus traffic flow for manual and automated traffic 27

Figure 2.9. Velocity profiles for a four vehicle platoon under CICC control 29

Figure 2.10. Acceleration profiles for a four vehicle platoon under CICC control 29

Figure 2.11. CO emissions versus time for a four vehicle platoon under CICC control 30

Figure 2.12. NOx emissions versus time for a four vehicle platoon under CICC control 30

Figure 2.13. Velocity profiles for a four vehicle platoon under perturbed CICC control 31

Figure 2.14. Acceleration profiles for a 4 vehicle platoon under perturbed CICC control ... 32

Figure 2.15. CO emissions vs. time for a 4 vehicle platoon under perturbed CICC control.. 32

Figure 2.16. NOx emissions vs. time for a 4 vehicle platoon under perturbed CICC control 33

Figure 2.17. Accumulative CO emissions for perturbed and non-perturbed control cases ... 33

Figure 2.18. Accumulative NOx emissions for perturbed and non-perturbed control cases . 34

Figure 2.19. Velocity profiles for a four vehicle platoon under AICC control 35

Figure 2.20. Acceleration profiles for a four vehicle platoon under AICC control 35

Figure 2.21. CO emissions versus time for a four vehicle platoon under AICC control…… 36

Figure 2.22. NOx emissions versus time for a four vehicle platoon under AICC control …. 36

Figure 3.1. Freeway geometry for FRESIM ramp meter experiment…… 40

Figure 3.2. Average mainline freeway speed vs. traffic volume on a non-metered ramp..… 41

Figure 3.3. Average mainline freeway speed vs. ramp meter cycle time …… 42

Figure 3.4. CO emissions rate per mile versus ramp meter cycle time…… 43

Figure 3.5. HC emissions rate per mile versus ramp meter cycle time…… 44

Figure 3.6. NOx emissions rate per mile versus ramp meter cycle time …… 44

Figure 3.7. Vehicle density versus ramp meter cycle time…… 45

Figure 3.8. Average vehicle speed on ramp versus ramp meter cycle time…… 46

Figure 3.9. Emissions versus ramp meter cycle time …… 46

Figure 3.10. Average wait time versus ramp meter cycle time…… 47

Figure 3.11. CO, HC and NO_X emissions for constant length and varying grade..…… 49

Figure 3.12. Velocity vs. time for zero grade, accelerating from 10 to 55 mph…… 49

Figure 3.13. Acceleration vs. time for zero grade, accelerating from 10 to 55 mph…… 50

Figure 3.14. Sample velocity profiles for example ramp from CalPoly study …… 51

Figure 3.15. Sample acceleration profile for example ramp from CalPoly study…… 51

TABLES

Table 2.1. Specifications of 1991 Ford Taurus …… 18

Table 2.2. Environmental constants used in calculations …… 19

1 Introduction

Two central research questions pertaining to air quality exist for Intelligent Transportation Systems (ITS): Potential vehicle emission reductions through the application of advanced technology, and potential induced traffic demand.

Potential Vehicle Emission Reductions—ITS has the potential to reduce vehicle emissions through several of its "technological bundles" (see, for example, (ITE 1990) for an overview of ITS). Advanced Vehicle Control Systems (AVCS) implemented at the vehicle level are intended to safely smooth traffic flow on the roadways by minimizing the stop-and-go effect of vehicles in congestion, and increase overall throughput. The heavy acceleration and deceleration components of vehicle trips can be eliminated, minimizing energy consumption and associated emissions of these vehicle operating modes. Advanced Traffic Management / Information Systems (ATMIS) will allow dynamic re-routing to take place on the roadway network, minimizing congestion and subsequently emissions. Further, navigational systems will allow users to reduce unnecessary driving and avoid congestion (SCAQMD 1993) .

Potential Induced Traffic Demand—In contrast, the implementation of some ITS technologies may lead to an increase of total vehicle miles traveled (VMT). If ITS allows smoother flow and higher speeds on the roadways, people may choose to live farther away from work while still commuting in the same amount of time—thereby increasing VMT. Farther, attractive trip-ends will become reachable, again increasing VMT. Further, advanced navigational technology may divert travelers from higher-occupancy modes such as buses and carpools to single-occupant vehicles. In general, if travel becomes easier due to advanced technology, VMT will likely increase.

In order to determine the impact of ITS on air quality, significant improvements must be made in traffic simulation and travel demand models by closely integrating vehicle emission models. Existing traffic, emissions, and planning models have been developed independently of each other and are difficult to integrate together when determining accurate air quality impacts. Current emission models (i.e., MOBILE, EMFAC (Maldonado 1991; Maldonado 1992; Eisinger 1993)) functionally relate emissions to average vehicle speed and density, and are not appropriate for analyzing ITS scenarios. Under ITS conditions, the dynamic behavior of vehicles will be very different compared to today's traffic conditions, upon which the current emissions models are based. As a result, *modal emissions data* (i.e., emissions data associated with vehicle

modes, e.g., idle, acceleration, cruise, deceleration, etc.) should be used with microscale traffic simulations to obtain more realistic results.

In this research, we have begun to evaluate the direct impact on vehicle emissions of ITS traffic operation. We concentrate on the actual implementations of proposed strategies, and do not consider the effect of potential induced traffic demand as outlined above. In this introduction, we first describe the problems associated with current emission models, particularly with their use in evaluating ITS scenarios. A description of transportation modeling and an integrated (transportation/emissions) approach are then briefly described, followed by a summary of the project tasks.

1.1 EMISSIONS MODELING

The common modeling approach (specifically the MOBILE model, developed by the US Environmental Protection Agency (EPA) (Eisinger 1993) and EMFAC, developed by the California Air Resources Board (CARB) (Maldonado 1991; Maldonado 1992)) used to produce a mobile source emission inventory is based on two processing steps, as shown in figure 1.1. The first step consists of determining a set of *emission factors* which specifies the rate at which emissions are generated, and the second step is to produce an *estimate of vehicle activity*. The emission inventory is then calculated by multiplying the results of these two steps together.

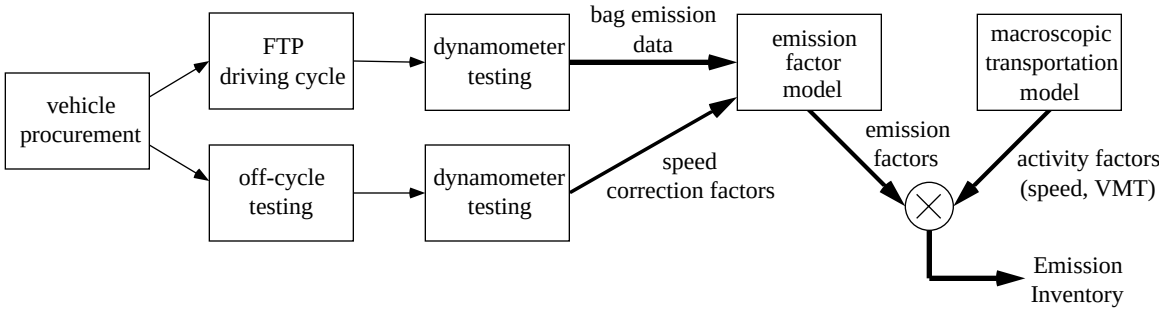

Figure 1.1. Current Emission Inventory Process

The current methods used for determining emission factors are based on laboratory-established emission profiles for a wide range of vehicles with different types of emission control technologies. The emission factors are produced based on average driving characteristics embodied in a pre-determined driving cycle, known as the Federal Test Procedure (FTP 1989) . This test cycle was originally developed in 1972 as a certification test and has a specified driving trace of speed versus time, which is intended to reflect actual driving conditions both on arterial roads and freeways. Emissions of carbon monoxide (CO), oxides of nitrogen (NO_x), and

hydrocarbons (HC) are integrated and collected for three sections of the cycle (called bags) and are used as base emission rates.

Adjustments are then made to the base emission rates through a set of correction factors. There are correction factors for each bag, which are used to adjust the basic emission rates to reflect the observed differences between the different modes of operation. There are also temperature correction factors and speed correction factors, used to adjust the emission rates for non-FTP speeds. These speed correction factors are derived from limited off-cycle testing (speeds greater than 57 mi/h (92 km/hr), accelerations greater than 3.3 mi/h-s (5.3 km/hr-s)) performed on laboratory dynamometers.

Vehicle activity data used for the emission inventory can come from a number of sources, although it is typically produced from a macroscopic transportation model. Traffic activity data is generated regarding vehicle miles traveled (VMT), number of vehicles, number of trips, and speed distribution on a region specific basis. Along with using an estimate of vehicle mix, the key variables of VMT and associated speed distribution are then multiplied with the emissions factors, producing a final emissions inventory. This methodology for calculating an emission inventory has several shortcomings, a few are outlined below:

1) **Inaccurate characterization of actual driving behavior** — One of the underlying problems is that the standardized driving cycle of the Federal Test Procedure, which is used to certify vehicles for compliance of emission standards and from which most of the emissions data are based, was established over two decades ago (FTP 1989) . At the time, the FTP was intended to exercise a vehicle in a manner similar to how a typical in-use urban vehicle would operate, however it did not include “off-cycle” vehicle operation which consist of speeds in excess of 57 mi/h and acceleration rates above 3.3 mi/h-s, common events in today’s traffic operation. It has been shown in a number of studies that the FTP does not accurately characterize today’s actual driving behavior (Cadle et al. 1991; Cadle et al. 1993) .

2) **The methodology of emissions factor calculation is flawed** — The non-representative nature of the FTP driving cycle tests is exacerbated by the procedure used for collecting and analyzing emissions. As mentioned before, the FTP is divided into three segments in which emissions are collected into separate bags. The emissions from these three segments are then used by the emission models to statistically reconstruct the relationship between emission rates and average vehicle speeds. Thus the models statistically smooth the effect of accelerations and decelerations. In simple terms, two vehicle trips can have the same average speed, but may have different speed profiles that consist of drastically different modal

characteristics (acceleration, deceleration, idle, etc.) and thus drastically different emissions output. This is particularly true for current closed-loop emission control systems where it has been shown that dynamic operations of the vehicle are an important variable in predicting vehicle emissions (Cadle et al. 1991; Cadle et al. 1993; St. Denis et al. 1993) .

Further, the speed correction factors used as the model input are derived from nine transient tests (not steady-speed tests) including the FTP. The tests span a series of average speeds up to 65 mi/h. Running the nine cycles and scaling them to construct the speed correction curves may not accurately mimic real-world driving conditions.

3) **Estimates of traffic activity lack sufficient depth and are often in error** — After emissions data have been collected through FTP testing, this data set is multiplied by the data produced by models of traffic activity. Unfortunately, the traffic density and vehicle speed information is out-of-date in most areas, VMT is consistently under-predicted (CARB 1991) , and traffic activity information has not been properly validated.

The technical community has recognized that vehicles are often operated at off-cycle speeds and accelerations, and several studies are on-going to better characterize in-use driving behavior and to obtain real-time, in-situ emission measurements (Cadle et al. 1991; Cadle et al. 1993) . Several instrumented vehicle projects are evaluating on-road vehicle performance by collecting real-time, in-situ vehicle operation parameters while simultaneously measuring emission data on a second-by-second basis (Butler 1992; Kelly et al. 1993) . With data from these instrumented vehicles, it is possible to examine the direct relationships between dynamic vehicle operation and emission output.

In addition, a new generation of chassis dynamometers has recently become available. Over the last several years, a joint task force comprised of EPA, CARB, and, at that time, the Motor Vehicle Manufacturers Association has investigated the feasibility of replacing the 8.65 inch twin-roll hydrokinetic chassis dynamometer with an electric dynamometer, for the purpose of improving system reliability and reducing emissions test variability. After several comparative programs it was found that a 48 inch single-roll electric dynamometer provided a better match to the road than the 20 inch twin-roll, coupled dynamometer. In addition, there were significant increases in emissions and a decrease in fuel economy using the 48 inch single roll dynamometer compared to the standard chassis dynamometer. Most importantly, the 48 inch single roll dynamometer allowed for the accurate testing of severe transient events (hard accelerations and decelerations greater than 6 mph/second) previously unattainable with the old generation dynamometers. The load applied to the vehicle can be dynamically controlled in real-time,

allowing the proper real-world simulation of road loads, aerodynamic drag, and road grade. By using emission analysis equipment capable of measuring emission species every second, again, the direct relationship between dynamic operation and emission output can be formulated with considerably increased accuracy.

With these instrumented vehicle projects and similar second-by-second dynamometer emissions tests, it is possible to improve our understanding of what types and what amounts of emissions are resulting in relation to the measured vehicle parameters, and build up a *modal* emissions data set, i.e., emissions as a function of vehicle operating modes, such as idle, light-, medium-, and hard-accelerations, steady -state cruise, etc. With these highly time resolved emission and vehicle data, modal emission models can be established so that given a certain set of vehicle operating conditions or modes, an instantaneous emission output can be predicted.

This is particularly important for the evaluation of various ITS scenarios, where driving conditions will not be similar to the conditions of the FTP, but rather be composed of diverse operating conditions that can only be evaluated using such a modal emissions modeling approach.

1.2 TRANSPORTATION MODELING

In general, transportation modeling consists of several integrated models that are used together to define the transportation planning process. These components are described in detail in the literature (e.g., Warner 1985)), and are briefly outlined below:

Trip Generation Models: This initial component is concerned with the causes of trips, i.e., what environmental circumstances lead to the production or attraction of traffic. This is usually based on demographic variables such as household size, income, and number of vehicles per household. Trip generation models estimate the number of total trips based on trip purpose on an area-by-area basis.

Trip Distribution Models: After estimating the traffic demand generated in each area, trip distribution models determine the destinations of the outflows and the origins of the inflows for the different areas.

Modal Choice Models: This component deals with what transportation modes will the anticipated flows use: private car, bus, train, etc. These models estimate the distribution of the transportation flows over the various transportation modes.

Trip Assignment Models: This final component is concerned with what route the transportation flows will take. With a network of different transportation routes, trip assignment models predict the paths of travel for the distribution of transportation flows. These network loading models usually are based on the assumption that users will always use the quickest route.

Once all of these components are in place, traffic can be simulated on a transportation network, usually composed of links and nodes. The links represent road segments and nodes represent potential turning points. Based on the demand database consisting of sources, destinations, volumes, and types of vehicles determined by the first three components described above, the traffic simulation predicts the traffic operation over the network as a function of time using the trip assignment component. The traffic simulation can illustrate such things as congestion due to inadequate road systems, construction, accidents, or similar factors.

Transportation simulation models typically fall into one of two categories, microscale and macroscale. Microscale models typically model at the vehicle level and have high accuracy, but require extensive data on the system under study and require more computing power than macroscale models for problems of the same scope. Macroscale models often require less detailed data, but they sacrifice detail in order to enable the modeling of larger areas using computers with modest power. Transportation simulation models are used for analyzing various operating environments of the road system. These operating environments include signalized intersections, arterial networks, freeway corridors, and rural highways.

Some examples of microscale performance models are TRAF-NETSIM (FHWA 1989, for arterial networks) and FRESIM (Halati et al. 1991, for the freeways) . Macroscale models that are based on analytic flow models include FREFLOW (May 1990) , TRANSYT-7F (FHWA 1986) and HCS (TRB 1985). Many of these models were developed before the introduction of efficient and cost-effective mini- and micro-computers. The models have been enhanced over the years, and many are powerful and effective. However, most are difficult to maintain and modify, contain bugs even after over a decade of development, and have rigid input/output routines structured around the punched card concept.

Therefore, newer traffic models are being developed in recent years that take advantage of the many developments of modeling, software engineering, and hardware platforms which have occurred over the past decade. For example, the THOREAU model (McGurrin et al. 1991) makes use of object-oriented programming for greater flexibility, and is based on event-stepped simulation rather than time-stepped, resulting in greater speed performance. Another recently developed transportation model is the model INTEGRATION (Van Aerde 1992) . These more

recent models are better suited for simulating various ITS scenarios, since they have greater flexibility and greater level of detail that are required for simulating new transportation technologies. Other specific transportation simulation models have been developed in particular for the evaluation of ITS, such as the simulators SmartPath (Eskafi et al. 1992; Hongola et al. 1993) and SmartLink (Rao et al. 1994) developed within the PATH program.

Few of these transportation models have been combined with vehicle emission models, and those that do simply predict vehicle density and speed as a function of link and time to be integrated with current speed-emissions data. Although this is a step in the right direction, much better emission estimates can be achieved using transportation models that can predict dynamic vehicle operating characteristics such as acceleration and deceleration, and combining these with a modal-based emissions model.

1.3 INTEGRATED TRANSPORTATION/EMISSION MODEL SUMMARY

As part of a larger research program, we are developing a new modeling approach for mobile source emission estimation, using a power demand-based modal emissions model, described in appendix A. This modal emissions model is being integrated with a set of transportation simulation models that attempt to portray true traffic behavior. By modeling in this fashion, emission rates are closely related to dynamic vehicle behavior and have the potential to provide a better overall estimate of total emissions. Because of the tight coupling between transportation simulation and modal emission modeling, we refer to our modeling set as the Integrated Transportation/Emission Modeling (ITEM) set (Barth et al. 1993) .

ITEM is based on a hybrid macroscale/microscale modeling approach, illustrated in figure 1.2. Detailed vehicle activity is determined through microscale simulation modules which are stratified by road facility type. A macroscale model (referred to as the wide area model) capable of simulating regional areas is then used to integrate all of the microscale simulation models together. There is strong interaction between the macroscale model and the microscale modules, indicated by two-way arrows in figure 1.2. Transportation parameters determined by the macroscale wide-area model are used to drive the input parameters of the modules. In addition, information sent back from the microscale modules is used as feedback to the wide-area model, which helps improve the system's overall traffic estimation.

Currently, ITEM has implemented an uninterrupted flow simulation model, which can simulate various levels of congestion on a freeway facility. Also, an acceleration module was developed to predict vehicle emissions directed related to specified velocity/acceleration profiles. Further,

an arterial congestion model is currently being developed, along with a rural highway model capable of predicting emissions for passing events.

At this stage of development, ITEM cannot be used to calculate a comprehensive mobile source emissions inventory. It operates at a high level of detail, however it currently lacks the breadth of emission measurements for a large range of vehicles, and can only simulate a limited range of traffic scenarios. Rather, this approach to emissions modeling attempts to avoid the potential problems and shortcomings of current emissions modeling and establishes a foundation for future emission inventory procedures.

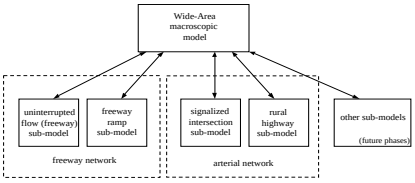

Figure 1.2. Hybrid macroscopic / microscopic modeling approach of ITEM.

1.4 PROJECT TASK OUTLINE

In the first year's work, the Integrated Transportation/Emission Modeling set has been enhanced so that several ITS scenarios can be evaluated. After the enhancement, initial studies of Advanced Vehicle Control System (AVCS) and Advanced Traffic Management and Information System (ATMIS) strategies have been performed. The specific tasks are outlined below:

1.4.1 Task 1: Transportation/Emissions Model Enhancement for ITS

In order to evaluate the effect on total vehicle emissions from specific ITS strategies, traffic simulation models are being integrated with the modal emission component of ITEM. In this first year, we have investigated vehicle emissions associated with two specific cases of ITS: 1) vehicle platooning that will take place within an Automated Highway System (AHS), and 2) ramp metering used to smooth the flow on the freeways.

Vehicle Platooning:

In an automated highway system, vehicles will most likely travel in platoons, where a platoon consists of a number of vehicles (approximately 5 to 30), separated by very short distances (on the order of a meter), traveling at high speeds (100 km/hr +). As a starting point, we have taken the microscale uninterrupted flow (freeway) simulation module of ITEM and modified it by eliminating the human driving behavior components corresponding to car-following and lane-changing logic. These components have been replaced with the control laws for automated driving. Two types of car-following logic within a platoon are being considered: 1) Coordinated Intelligent Cruise Control (CICC) where a platoon leader has a rearward-looking transponder or other means of transmitting information on vehicle dynamics to the following vehicles, and 2) Autonomous Intelligent Cruise Control (AICC) where a following vehicle can only measure a preceding vehicle's position and velocity. These control laws are being adapted from the PATH literature, specifically (Sheikholeslam 1991) for CICC and (Ioannou et al. 1992) for AICC. In addition, the graphical user interface for the simulations is being modified for platoon generation. The AHS simulator SmartPath (Eskafi et al. 1992; Hongola et al. 1993), developed within PATH, is being evaluated to determine whether the simulator can be used for emissions analysis.

Ramp Metering:

In addition to evaluating vehicle platooning emissions, we are analyzing the effect of advanced traffic management; specifically, the effect of ramp metering on vehicle emissions. Ramp metering has three basic effects on vehicle emissions: 1) smoothing of freeway traffic, leading to lower emissions, 2) increased ramp and surface street congestion, possibly leading to higher emissions, and 3) induced hard accelerations from the meters on the ramps, leading to higher emissions.

These three effects are obviously interrelated and vary as a function of traffic demand, ramp meter cycle time, and ramp meter placement. In this first year of work, these three effects have been modeled and evaluated *independently* with no interaction between them. A large concentration of work has been on the induced hard accelerations. The ramp-acceleration module of ITEM has been adapted to predict the amount of vehicle emissions during hard accelerations on freeway on-ramps. These ramp accelerations have been compared to data measured in the 1993 Caltrans project "Vehicle Speeds and Accelerations Along On-Ramps: Inputs to Determine the Emissions Effects of Ramp Metering" performed by Cal Poly (Sullivan et al. 1993) .

1.4.2 Task 2: Initial Study of AVCS Strategies

As an initial study of AVCS strategies, total emissions from platoons in an AHS scenario have been evaluated. Specifically, the following evaluations have been conducted:

Steady-state speed/emissions comparison—The emissions for a 20 vehicle platoon are calculated at different steady state speeds. These emissions are then compared to 20 vehicles driven manually (i.e., no platooning), with no intervehicle interaction for the same set of velocities. Due to the reduction of aerodynamic drag while platooning (the "drafting" effect), the emissions for the platoon are significantly lower at higher steady-state speeds.

Optimized vs. non-optimized CICC comparison—A comparison has been made between a platoon under optimized and non-optimized CICC control laws. In the optimized case, control constants are set at their optimized values for best maintaining intraplatoon spacing. For the non-optimized case, these control constants are perturbed and the resulting emissions are compared to the optimized case. At high speeds under high load conditions, the non-optimized case tends to produce higher emissions.

CICC vs. AICC comparison—Various driving cycles (velocity profiles of on-road vehicle motion) have been simulated for both CICC and AICC platoon operation. Although platoons will be operated smoothly in a typical AHS, more aggressive driving cycles were used in simulation in order to identify potential emission producing events. For specific velocity transients, hard accelerations and decelerations were often required of follower vehicles to maintain proper platoon formation. These accelerations often lead to short bursts of high emissions during the driving cycles, depending on the control laws governing intraplatoon spacing. A comparison of total emissions have been carried out using CICC and AICC control laws.

A description of this preliminary AHS evaluation is given in chapter 2.

1.4.3 Task 3: Initial Study of ATMIS Strategies

An initial evaluation has been conducted of ramp metering and its effect of vehicle emissions. Three components of ramp metering were evaluated independently: 1) The effect of freeway traffic smoothing; 2) Ramp and surface street congestion; and 3) Hard accelerations from the ramp meters. The freeway smoothing effect has been evaluated using the model FRESIM (Halati

et al. 1991) for different scenarios of ramp metering. Ramp congestion has been analyzed using a microscale simulation model of a single lane ramp. The ramp-acceleration module of ITEM has been adapted to predict the amount of emissions during hard accelerations on freeway on-ramps.

A description of this preliminary ramp metering evaluation is given in chapter 3.

2 Automated Highway System (AHS) Vehicle Emissions

Automated Highway Systems (AHS) offer the potential for a substantial increase in performance and safety on the nation's highways. Research conducted at PATH has shown conceptually that an AHS can provide safe, efficient movement of vehicles on the highway (e.g., Karaaslan et al. 1990; Varaiya et al. 1991; Rockwell 1992; Zhang et al. 1994) . However, an AHS is a complex system and must be capable of performing a wide range of operations, such as network traffic management, route planning and guidance, coordination of vehicle movements, and automated vehicle maneuver control. Each of these operations will have an effect on vehicle emissions.

In this research project, we have begun to evaluate the impact of AHS on vehicle emissions using simulation modeling. In this first year, we have concentrated on automated vehicle control, specifically on the operation of "platooning" implemented using longitudinal control. A fully automated highway system will consist of automated traffic in several lanes using both longitudinal and lateral control, with numerous platoon maneuvers such as platoon splitting, merging, etc. (see, e.g., Hsu et al. 1991; Varaiya et al. 1991). The impact of these maneuvers on vehicle emissions is not considered in this first year's work, but will be addressed in the second year using more sophisticated simulation models.

Principles of uninterrupted traffic flow are first reviewed, followed by a brief description of platooning concepts. A platoon simulation model developed in this first year's work is then described. Using the platoon simulation model, steady-state emissions are evaluated and compared to manual traffic emissions, followed by a preliminary analysis of transient emissions from platooned vehicles.

2.1 UNINTERRUPTED TRAFFIC FLOW

Current highway traffic (i.e., uninterrupted traffic flow) can be characterized by the traffic volume (v), average vehicle speed (S), and vehicle density (D). These terms are generally related by the product $v = S \times D$ (TRB 1985) . Further constraints operate on these parameters which restrict the type of flow conditions on a highway link. The general form of these constraints is shown in figure 2.1, which illustrates some key points of uninterrupted traffic flow:

- Zero rate of flow occurs in two distinct cases: 1) when there are no vehicles on the roadway, and 2) when the density is so high that all vehicles are stopped and cannot move. In the first case, the density is zero, thus the flow rate is zero, and the speed in this case is assumed to be the driver's desired speed (i.e., vehicle free speed). In the second case the density is at its

maximum and the vehicle speed is zero. The density at which this occurs is called the jam density.

- As density increases from zero, the traffic flow increases due to the increased number of vehicles. The average vehicle speed is reduced to maintain safety during higher density conditions.

- Traffic flow is maximized at a specific critical density. As density increases above the critical density point, speed drops off at a faster rate. Traffic flow tends to become unstable in this region due to perturbations from lane change maneuvers, merging, or any external variables (e.g., debris in roadway, accident in adjoining roadway, etc.). These perturbations can create disturbances that are not damped or dissipated in the flow. These unstable, forced flow regions in the curves are characterized by stop-and-go congestion.

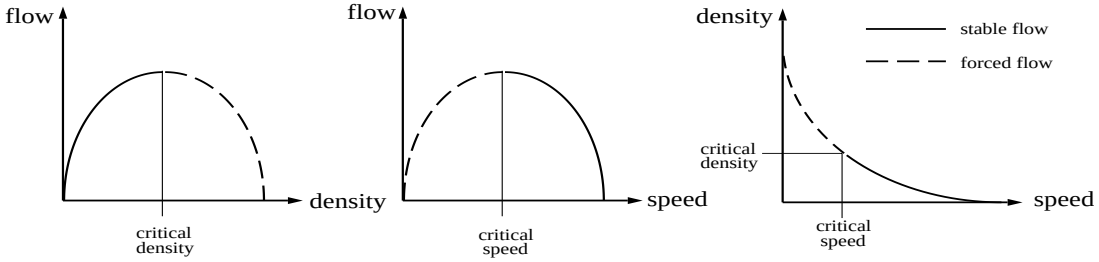

Figure 2.1. Flow, density, and speed relationship of uninterrupted traffic flow.

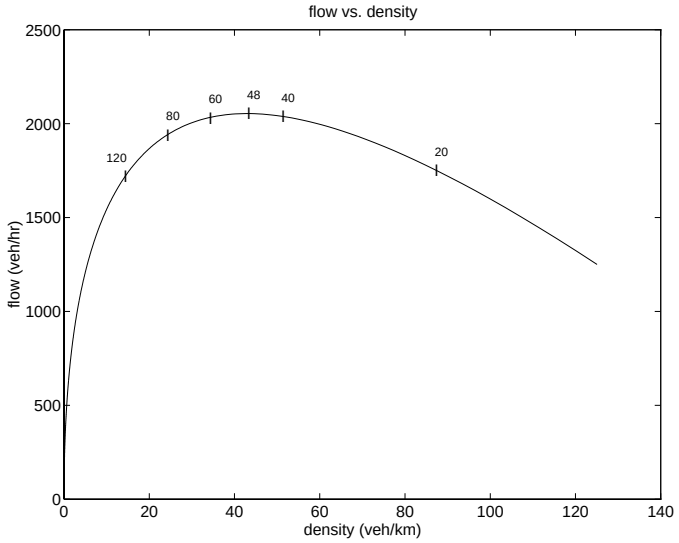

Figure 2.2. Flow-density relationship for manual traffic. Velocity values (km/hr) are annotated on the curve.

Human driver flow-density-speed relationships can be approximated mathematically by specifying the spacing, or gap, between vehicles required for safe stopping if one car suddenly brakes, and after a time lag, the second car also brakes without collision. The flow-density curve in figure 2.2 was produced for the case when the first car brakes at 0.9 g (8.82 meters/second^2) and the second car brakes at 0.6 g (5.88 meters/second^2) after a one second time lag. This curve (after Rockwell 1992) is for a single lane and is similar to curves predicted by the Highway Capacity Manual (TRB 1985) .

2.2 PLATOONING

In order to improve the flow rate on the highway, ITS technology in the form of AVCS can be applied to control vehicle motion so that vehicles can operate in platoons, i.e., follow each other very closely at high speeds, while still maintaining a high safety margin. This has several implications: 1) traffic flow will increase dramatically over current highway conditions due to denser traffic traveling at higher speeds; 2) congestion should decrease since the stop-and-go effect caused by relatively long human reaction delays will be eliminated and accidents will be minimized.

A similar mathematical formulation to that above can be developed for the flow-density-speed characteristics of an automated highway system. Within a platoon of vehicles, the spacings are much smaller and closely regulated by automated controls. Therefore, platooned vehicles can travel faster at higher densities, thus improving the traffic throughput. If we consider a single lane of platooned traffic as shown in figure 2.3, we can mathematically approximate the flow-density-speed characteristics. Using the notation given in figure 2.3, the vehicle density for an automated lane is given as:

$$D = \frac{n}{\Delta + n(L + \delta) - \delta} \tag{2-1}$$

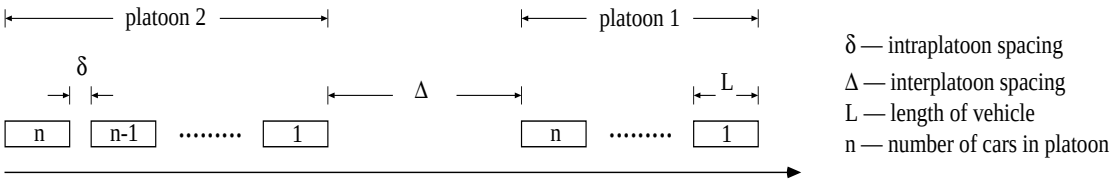

Figure 2.3. Platoons of vehicles on a highway.

The interplatoon spacing is determined as described before, i.e., requiring safe stops if one platoon suddenly brakes, and after a time lag, the second platoon (leader) also brakes. In the automated scenario, the time lag is much shorter than that for human drivers. The resulting flow-density curve in figure 2.4 was produced for the more restrictive case when the first platoon brakes at 2 g (19.6 meters/second^2), and after a 0.3 second time lag, the second platoon (leader) brakes at 0.3 g (2.94 meters/second^2). It is assumed that the intraplatoon spacing is precisely controlled and can also perform safe stops under these specified stopping conditions. In the mathematical formulation, the intraplatoon spacing is set to one meter, the car length is five meters, the number of vehicles in each platoon is 20 vehicles, and the vehicle free speed is 120 km/hr. The difference between the flow for manual driving and automated driving is substantial. The maximum traffic flow for this automated case is roughly four times that of the manual driving case. The maximum flow for the automated case occurs at an average speed of 103 km/hr, and for the manual case it occurs at 48 km/hr.

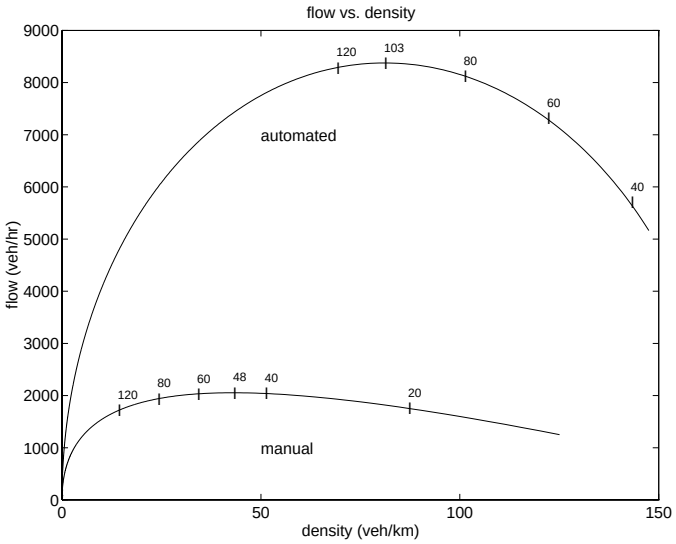

Figure 2.4. Flow-density relationship of traffic for both manual driving and automated driving. Velocity values (km/hr) are annotated on the curves.

2.3 PLATOON SIMULATION MODEL

In order to study the emissions effect of vehicles traveling in platoons, a computer simulation model was developed. This microscale platooning model simulates individual vehicle behavior on a freeway and integrates each vehicle's calculated operating parameters to determine an emissions output, based on modal emissions model described in appendix A. Although multiple lanes have been implemented in the simulation, control has been implemented only in the longitudinal direction; lateral control for lane changing, platoon merging, and platoon splitting have not been implemented.

2.3.1 Vehicle Dynamics

This simulation model considers at the fundamental level each vehicle's acceleration performance. The acceleration performance (in the longitudinal direction) is limited by the engine power and the traction limits on the drive wheels. Engine power is modeled in detailed using torque curves that vary with RPM (Gillespie 1992) . For a more detailed estimation of engine power transferred to the road, a power train model was also developed. Vehicle acceleration due to engine power is modeled as follows (from Gillespie 1992) :

$$a_{ep} = 76.2 \frac{\mathrm{g} \times HP}{V \times \mathrm{W}} \tag{2-2}$$

where g is the gravitational constant (9.8 m/sec^2), HP is the engine horsepower, V is the vehicle velocity (m/sec) and W is the weight of the vehicle (kg). The constant 76.2 converts from horsepower to m-kg/sec. This is the vehicle's acceleration, given in m/sec^2, due only to engine power.

The effect of rolling resistance is based on the equation (after Gillespie 1992) :

$$a_{rr} = -f_r \times \mathrm{g} \tag{2-3}$$

where f_r is the rolling resistance coefficient, and again g is the gravitational constant. Note that this term is negative since the resistance results in negative acceleration. This rolling resistance coefficient takes into account energy due to deflection of the tire sidewall near the contact area, energy loss due to deflection of the road elements, scrubbing in the contact patch, tire slip in the longitudinal and lateral directions, deflection of the road surface, air drag on the inside and outside of the tire, and energy loss on bumps (Gillespie 1992) . Changes in vehicle weight alters this relationship, but not significantly and therefore will not be considered.

The effect of aerodynamic drag on acceleration is significant at high speeds. The drag depends on the dynamic pressure, and is proportional to the square of the speed. Acceleration loss due to aerodynamic drag is given as (Gillespie 1992) :

$$a_{ad} = -\frac{\rho}{2} \times \frac{\mathrm{g}\, C_D\, \mathrm{A}\, V^2}{\mathrm{W}} \tag{2-4}$$

where ρ is the air density, C_D is the aerodynamic drag coefficient, A is the frontal area of the vehicle, W is the vehicle weight, and V is the vehicle velocity. Again, this is a resistive force to the vehicle, and thus the acceleration is negative.

Because the follower vehicles within a platoon have very small intraplatoon spacings (e.g., on the order of one meter), the aerodynamic drag coefficient of each follower is significantly reduced due to the "drafting effect" (Zabat et al. 1993) . Using preliminary aerodynamic drag reduction data for vehicles in platoons (Zabat et al. 1993) , the calculated load on the engine is significantly smaller at higher speeds. Based on the data, even the lead vehicle of a platoon has its aerodynamic drag coefficient reduced due to the vehicle following closely behind. Therefore, when a vehicle travels in a platoon in the simulation, the aerodynamic drag coefficient is reduced by an adjustment factor derived from the results of (Zabat et al. 1993).

Finally, the influence of road grade on acceleration is considered. This is a simple relationship which depends on the sine of the grade angle:

$$a_{rg} = -\mathrm{g} \times \sin(\theta) \tag{2-5}$$

If all of these equations are now put together to get the total vehicle acceleration, the result is:

$$\begin{aligned} a_{total} &= a_{ep} + a_{rr} + a_{ad} + a_{rg} \\ &= 76.2\frac{\mathrm{g} \times HP}{V \times \mathrm{W}} - f_r \times \mathrm{g} - \frac{\rho}{2} \times \frac{\mathrm{g}\, \mathrm{C}_{\mathrm{Dadj}}\, \mathrm{A}\, V^2}{\mathrm{W}} - \mathrm{g} \times \sin(\theta) \end{aligned} \tag{2-6}$$

where C_{Dadj} is the adjusted aerodynamic drag coefficient due to drafting within the platoon. With this equation, it is possible to determine acceleration as a function of velocity, along with several constants.

In the simulation, each vehicle was modeled as a 1991 Ford Taurus, which has the following characteristics:

maximum horsepower	140 hp
weight	2020 kg
rolling resistance coefficient	0.015
aerodynamic drag coefficient	0.42
frontal area	3.1 m^2

Table 2.1. Specifications of 1991 Ford Taurus.

These values are combined with the following constants:

gravitational constant g	9.8 m/sec^2
air density ρ	0.00236
grade θ	0°

Table 2.2. Environmental constants used in calculations.

The vehicle dynamics of coasting (little or no engine power applied) are based on the rolling resistance and aerodynamic forces applied to each vehicle. The coasting acceleration (which is negative in this case, a deceleration) is given as:

$$a_{coast} = -f_r \times \mathrm{g} - \frac{\rho}{2} \times \frac{\mathrm{g}\, C_D\, A\, V^2}{W} - \mathrm{g} \times \sin(\theta) \tag{2-7}$$

The vehicle dynamics of braking are also considered, where it is assumed that a constant braking force F_b is applied to the vehicle, resulting in negative acceleration. Thus, a braking term is introduced in the acceleration equation:

$$a_{brake} = \frac{F_b \times g}{W} - f_r \times \mathrm{g} - \frac{\rho}{2} \times \frac{\mathrm{g}\, C_D\, A\, V^2}{W} - \mathrm{g} \times \sin(\theta) \tag{2-8}$$

F_b is the total of all braking forces, i.e., front axle braking force, rear axle braking force, and engine braking. If F_b exceeds a certain threshold, then wheel lockup occurs, and the vehicle deceleration is dependent on the effective coefficient of friction at the tire-pavement contact surface.

2.3.2 Longitudinal Control

In the simulation, it is assumed that longitudinal control for a platoon lead vehicle is based on the car following equation* :

$$\ddot{x}_{n+1}(t + \Delta t_{n+1}) = S_{n+1} \frac{[\dot{x}_n(t) - \dot{x}_{n+1}(t)]}{[x_n(t) - x_{n+1}(t)]} \tag{2-9}$$

where Δt_{n+1} is the *reaction delay* of vehicle n+1 and S_{n+1} is the *sensitivity* of vehicle n+1. Note that this equation bases the acceleration directly proportional to relative velocity (originally from Forbes' theory (May 1990)) and inversely proportional to the distance headway (originally from

* The longitudinal control of the platoon lead vehicle will likely be automated, using information based on link characteristics. However, in order to simulate safe gaps between platoons, a simple car-following equation is used.

Pipes' theory (Pipes 1953)). The sensitivity and reaction delay factors are stochastically assigned based on Gaussian probability densities derived from the literature (Barth et al. 1993) .

Longitudinal control for a follower vehicle in a platoon has been implemented using control laws for Coordinated Intelligent Cruise Control (CICC), and Autonomous Intelligent Cruise Control (AICC). The CICC algorithm is based on the work carried out by Desoer and Sheikholeslam (see, e.g., Sheikholeslam 1991) for the PATH program. The AICC algorithm is based on the work carried out by Ioannou et al. (Ioannou et al. 1992).*

2.3.3 Platoon Generation

The microscopic platoon model simulates a highway link that has a specified length, a specified number of lanes, and a specific grade. Given these input parameters, platoons are generated independently in each lane. The simulation models the generation of platoons on each lane as a modified Markov process. In a normal Markov process, times between generations have an exponential distribution with infinite support. In order to avoid extreme behavior in the simulation, inter-generation times which are extremely high (above five standard deviations) are eliminated and the remaining sample is shifted accordingly.

The generation rate is given by:

$$T_{next} = -1.0349 \times \frac{\log(u) \times \text{mtbg}}{V_{master}} \tag{2-10}$$

where T_{next} is the calculated generation time, u is a uniformly distributed random variable between 0 and 1, mtbg is the mean time between generations of vehicles set by the front control panel of the simulation, and V_{master} is a master volume constant for calibration (normally at 1).

2.3.4 Simulation Flow

The simulation flowchart is shown in figure 2.5. The simulation begins with the specified parameters of number of lanes, input density and speed, output density and speed, link length, and link grade. The simulation is first initialized, checking input from the front panel. Execution is halted if the quit button is pushed. The simulation has a master clock or simulation clock which is initially compared to the simulation time, or length of the current simulation. Platoons

* The details of these control algorithms are extensive and thus are not given here. The reader is referred to the corresponding citations for each control algorithm.

can be generated manually or by an independent process, and if it is time to generate a platoon in any lane, the simulation processes the platoon leader generation. In the generation process, initial acceleration and velocity parameters are determined, after which the behavior parameters are set. At the end of the generation process, the next platoon generation time in the current lane is scheduled.

Beginning with the first vehicle in each lane, the simulation runs through and updates each vehicle. Each lane is considered simultaneously, i.e., vehicles are updated based on their longitudinal position on the road, not just within their lane. If the current position of a vehicle is beyond the link length, then that vehicle is deleted from the vehicle list, and the updates continue with the next vehicle. When updating a vehicle, the car-following logic described previously is assigned for platoon leaders, or if a follower vehicle, the automated control algorithm is used. This updating continues until the last vehicle is updated. The simulation clock is then incremented, and the process repeats.

This is an event-based simulation that schedules vehicle generations based on the generation process described above. The incrementing of the simulation is also based on events, where each update occurs at predetermined update rate. The current update rate is every 100 milliseconds.

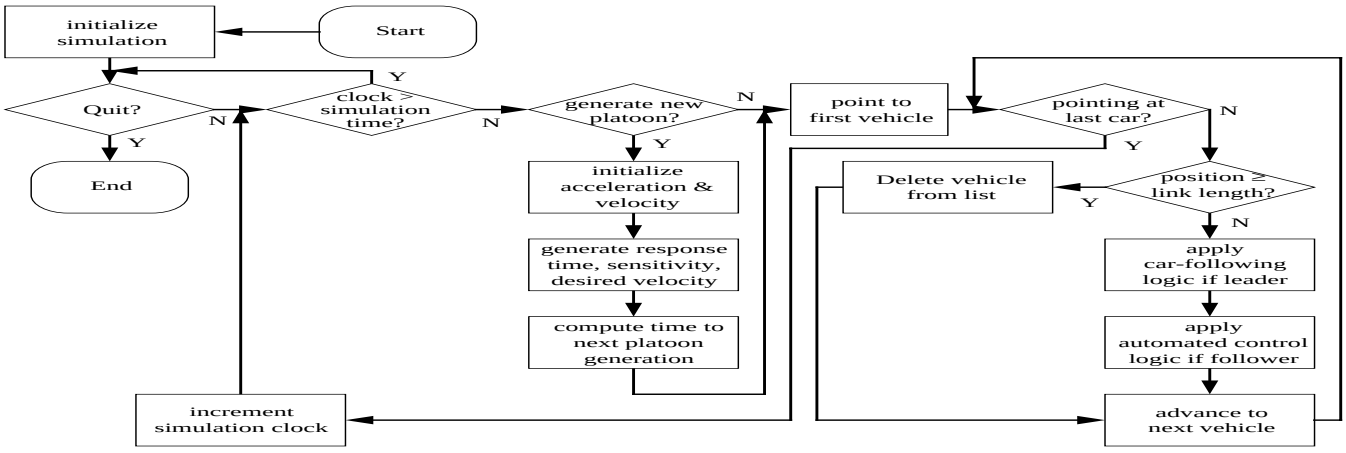

Figure 2.5. Overall flowchart of platoon simulation.

2.3.5 Graphical User Interface

The graphical user interface of the platoon simulation model is shown in figure 2.6. The controls of the simulation are on the left, and the view area of the simulation is shown on the right. In the view area, platoons of vehicles are generated on the lanes starting in the upper left corner. The lanes go left to right, and wrap around to the next level. The vehicles reach the end of the link in the lower right corner, where they disappear from the screen. The link can also be made circular so that platoons continue from the end of the link back onto the beginning of the link. The roadway and platoons are represented with 3D graphics and can be viewed from any 3D vantage point. The 3D is useful to see the effect of road grade. The colors of the vehicles indicate whether a vehicle is a platoon leader or a follower vehicle.

The simulation clock is shown in the upper right of the control section, followed by second-by-second emission values for CO, HC, and NO_x. The emission values are given as link totals and as average vehicle values. The density and average speed of the link are also shown. The simulation time is controlled by the sampling interval, and the delay factor determines how quickly the simulation runs. The size of the platoon can be set manually, or set randomly within the simulation. The leader velocity of each platoon can be set via an external driving cycle file, or can be controlled manually by selecting the platoon and using the leader velocity slider.

The type of control (i.e., AICC, CICC) for the platoons can be selected with the platoon type button. Platoons can be generated manually with the platoon generation button, or can be generated randomly within the simulation. Buttons near the bottom allow the simulation to advance, halt, pause, restart, and clear. The entire simulation can be stopped with the quit button.

2.4 STEADY-STATE SPEED EMISSIONS

In order to determine emissions associated with platooning, we first only consider steady-state vehicle speeds and the associated emissions. Traffic at steady-state speeds implies that there is little or no traffic interaction, vehicles are traveling near their assigned free speeds, and there are no variations in velocity (i.e., no congestion stop-and-go).

Using the power-demand emissions model in conjunction with the platoon simulator described earlier, experiments were carried out to determine average emission rates of platoons at different steady-state velocities. Emissions from a platoon of 20 vehicles are compared directly to that of 20 non-platooned vehicles (i.e., manually driven vehicles). The emission rates at different velocities are shown in figures 2.7a, 2.7b, and 2.7c.

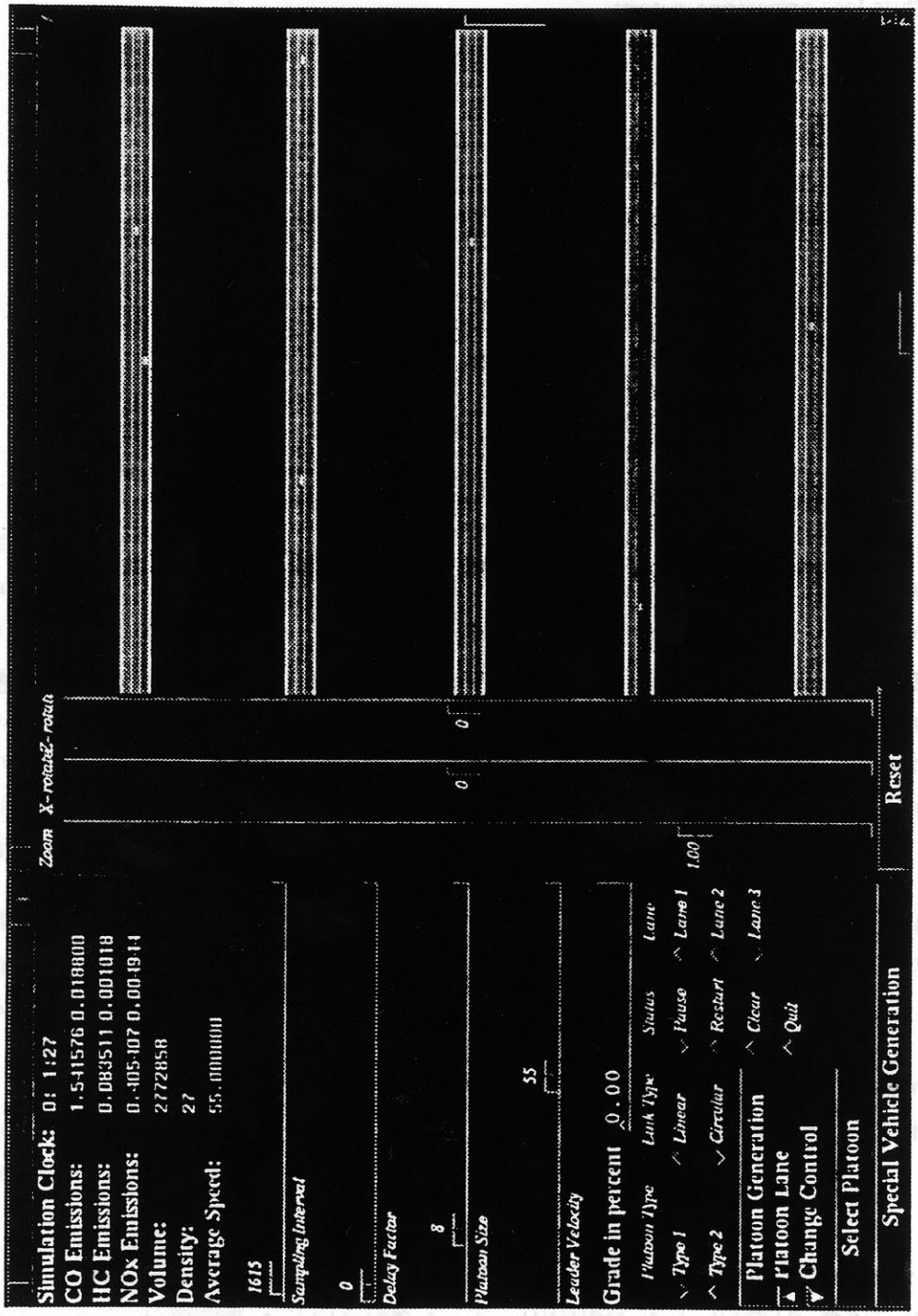

Figure 2.6. Graphical user interface of platoon simulation.

At lower speeds, vehicle emission rates of the two cases are roughly the same. However, at higher speeds, the platooned vehicles benefit from the drafting effect which results in less engine load, and thus less emissions output.

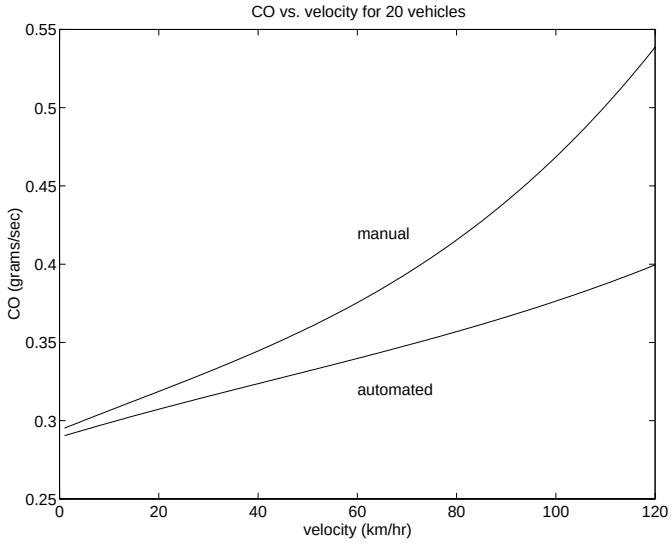

Figure 2.7a. Constant velocity CO emission rates for 20 vehicles platooned and non-platooned.

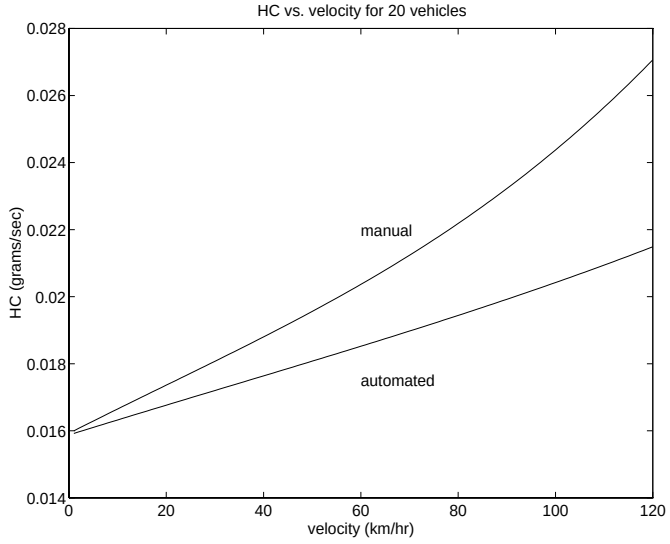

Figure 2.7b. Constant velocity HC emission rates for 20 vehicles platooned and non-platooned.

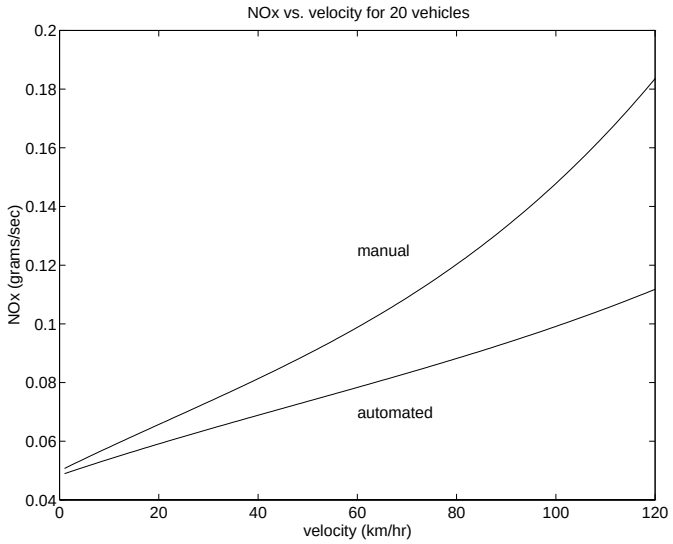

Figure 2.7c. Constant velocity NO_x emission rates for 20 vehicles platooned and non-platooned.

In order to determine total steady-state emissions of an automated lane within an AHS, these emission data were applied to the flow-density curves shown in figure 2.4. It is important to note that the curves in figure 2.4 reflect traffic density and flow associated with specified safe spacings. Thus to generate flow values at lower densities, vehicle speeds greater than the free speed (i.e., the maximum speed a driver will go on the freeway without interference from other traffic) were used in the calculations. For purposes of generating total link emissions at lower densities, the flow values were adjusted so that the vehicle velocities at low densities were at the constant free speed.

Total CO, HC, and NO_x emissions for a one kilometer lane are shown as a function of traffic flow for both the manual and automated (platooning) cases in figure 2.8a, 2.8b, and 2.8c respectively. There are several key points to note in these figures:

1) The maximum traffic flow for a manual lane is 2053 vehicles/hour at an average vehicle speed of 48 km/hour. At the same traffic volume, the automated lane produces roughly *half* as much emissions as in the manual case:

	CO (gm/s)	HC (gm/s)	NO_x (gm/s)
manual	0.76	0.0415	0.1882
automated	0.34	0.0174	0.0911

2) Given the emissions rate for maximum manual traffic volume, roughly *twice* the traffic volume can occur in the automated lane to produce the same amount of emissions:

	flow - CO	flow - HC	flow - NO_x
manual	2053	2053	2053
automated	4565	4601	4041

3) The maximum traffic flow for an automated lane is 8286 vehicles/hour at an average speed of 103 km/hour. The associated emissions at this point is roughly *twice* that of the maximum flow rate of manual driving:

	CO (gm/s)	HC (gm/s)	NO_x (gm/s)
manual	0.76	0.0415	0.1882
automated	1.5435	0.0837	0.4103

It is important to point out that the emissions associated with higher traffic densities and lower average speeds for the manual case are underestimated in these curves. Remember that these emissions are calculated based on steady-state velocities, and the negative slope region of the flow-density curve is inherently unstable, leading to stop-and-go traffic. The accelerations associated with stop-and-go traffic will lead to a greater amount of emissions.

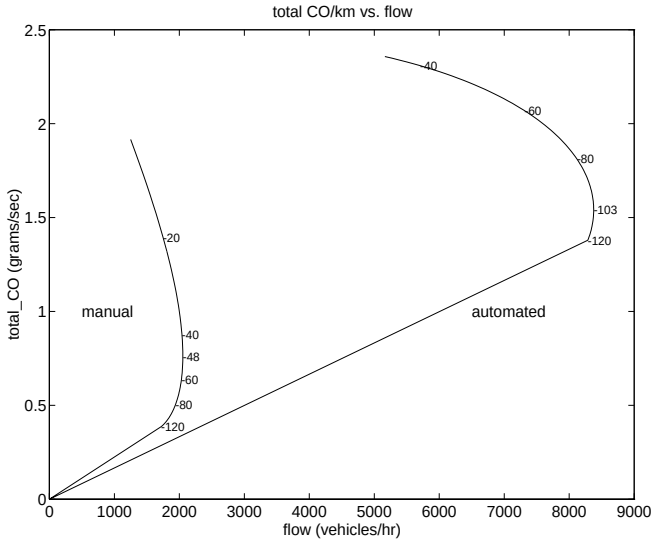

Figure 2.8a. Total CO emissions versus traffic flow for manual and automated traffic, for a one kilometer lane. Velocity values (km/hr) are annotated on the curve.

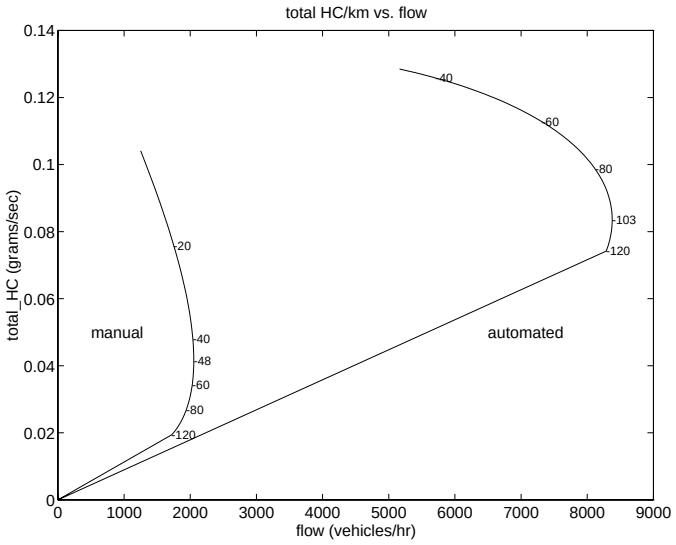

Figure 2.8b. Total HC emissions versus traffic flow for manual and automated traffic, for a one kilometer lane. Velocity values (km/hr) are annotated on the curve.

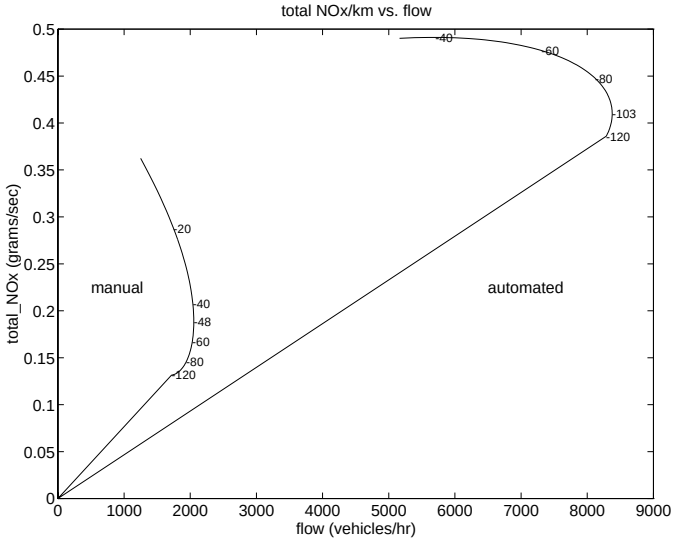

Figure 2.8c. Total NO_x emissions versus traffic flow for manual and automated traffic, for a one kilometer lane. Velocity values (km/hr) are annotated on the curve.

2.5 TRANSIENT VELOCITY EMISSIONS

In addition to emissions produced during steady-state velocity conditions, emissions produced during velocity transients are also considered. Using the platoon simulation model, a large number of simulations were carried out with different platoon lengths, different road grades, and different velocity profiles for the two different control algorithms, CICC and AICC. Initially, the Federal Test Procedure (FTP) driving cycle was applied to a platoon. Because the FTP driving cycle is not very severe in terms of vehicle performance (maximum acceleration 3.3 mph/sec, maximum speed, 56 mph), vehicles within a platoon were able to follow the prescribed driving trace with very little velocity deviation. As a result, there were no significant acceleration spikes leading to spikes in emissions output.

Although platoons will be operated smoothly in a typical AHS, more aggressive driving cycles were applied to platoons in the simulation model in order to identify potential emission producing events. An example of a more rigorous driving cycle is shown in figure 2.9. In this figure, the cycle consists of an overall acceleration from a velocity of 0 mph to 100 mph, followed by a deceleration back down to 10 mph. During the acceleration, there are plateaus where the velocity levels off at 20, 40, 60, and 80 mph for a few seconds. The acceleration was performed at an engine load value approximately 70% of the modeled vehicle's maximum horsepower. The acceleration segments are naturally steeper at lower speeds due to lower resistance terms that are functions of velocity (i.e., rolling resistance, aerodynamic drag).

Figure 2.9 shows the velocity profiles for each vehicle in a four car platoon, following the prescribed driving trace. It is apparent that the vehicles track very well in this CICC implementation (Sheikholeslam 1991) . Only at the velocity transient regions (i.e., the regions where velocity changes sharply) are there small deviations in the velocity profiles. This is more readily apparent in figure 2.10, where the acceleration of each vehicle is plotted versus time. The maximum acceleration spike in this example driving trace is approximately one mph/sec above the prescribed acceleration value of the lead vehicle.

Instantaneous emission values were also calculated during this simulation example. CO emissions are shown as a function of time in figure 2.11[*] . It can be seen that the acceleration spikes seen in figure 2.10 correspond with the CO emission spikes. The overall CO (and HC)

[*] Hydrocarbon (HC) emissions have the same general response as carbon monoxide, different only by a scale factor. Therefore, HC emissions are not shown.

emissions are fairly low, and the spikes in the emission are less than 10% of the total emission rate. NO_x emissions versus time are shown in figure 2.12, having the same general response as CO.

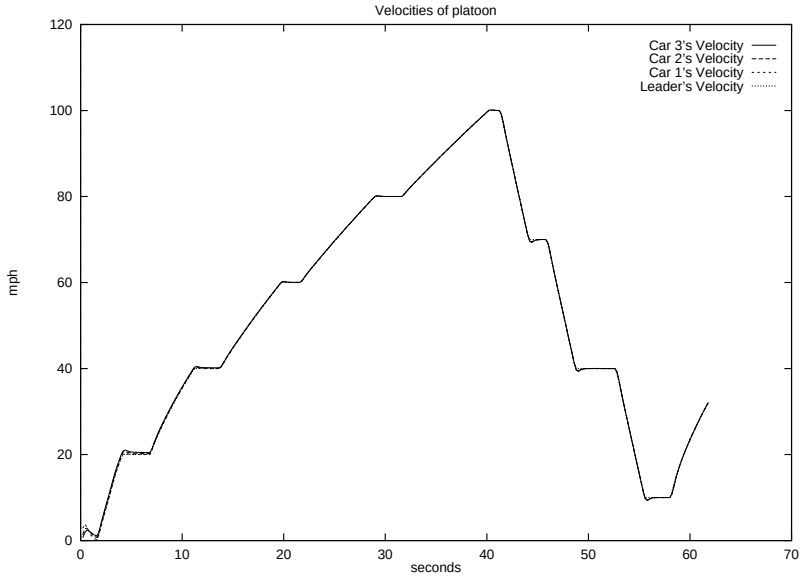

Figure 2.9. Velocity profiles for a four vehicle platoon under CICC control.

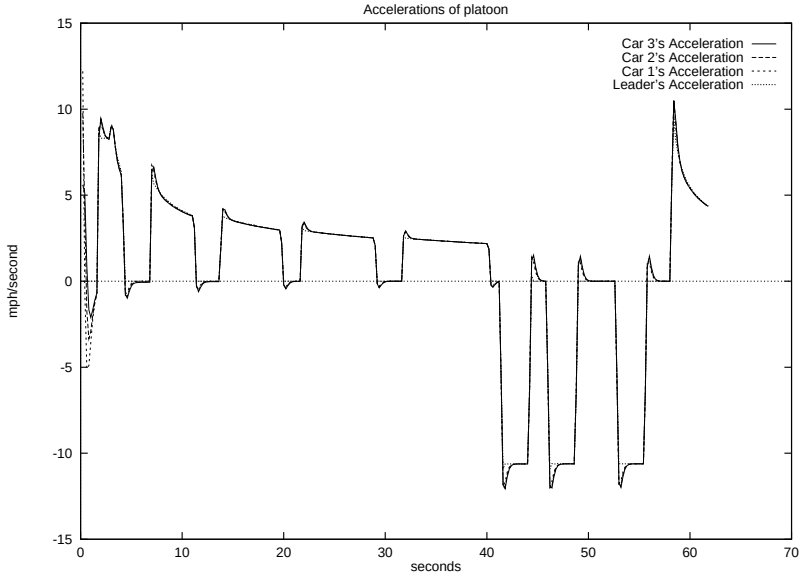

Figure 2.10. Acceleration profiles for a four vehicle platoon under CICC control.

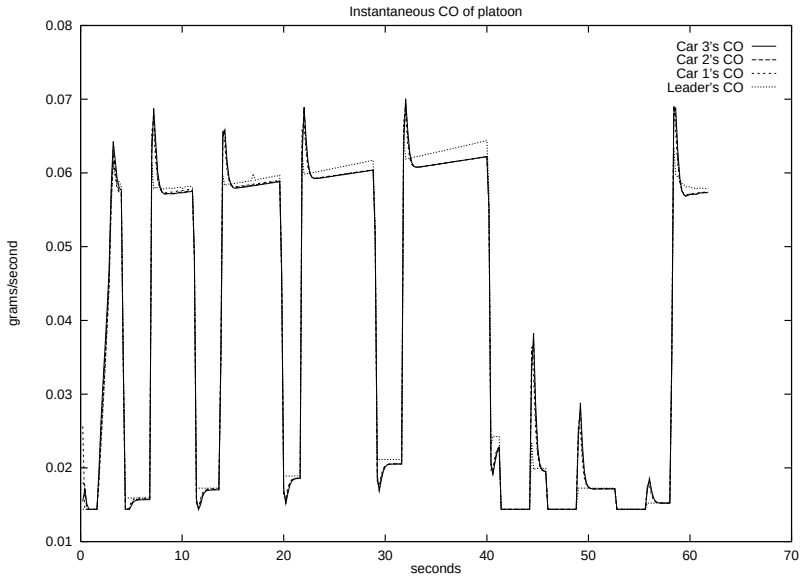

Figure 2.11. CO emissions versus time for a four vehicle platoon under CICC control.

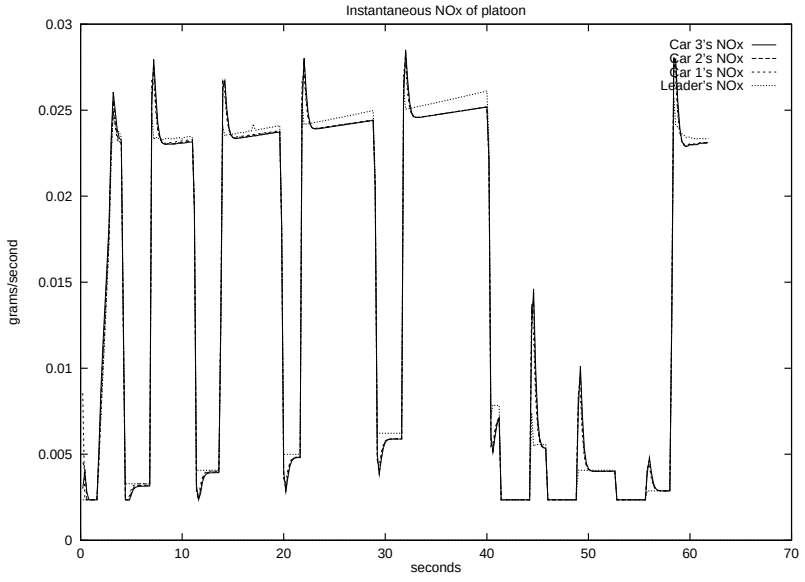

Figure 2.12. NO_x emissions versus time for a four vehicle platoon under CICC control.

2.5.1 Optimized vs. Non-Optimized CICC Comparison

The same driving trace was applied to a four vehicle platoon, however, the control laws governing how a follower vehicle maintains its intraplatoon headway were perturbed. The

control equations consist of several design constants that are set based on an optimal set of criteria for maintaining precise headway with as small as possible oscillations (Sheikholeslam 1991) . These control constants were slightly changed so that oscillations appeared in the control response; however, safe headways were still maintained.

The velocity profiles for each vehicle are shown in figure 2.13, where it is apparent that oscillations occur at velocity transient regions (compare this directly to figure 2.9). This is shown more clearly in figure 2.14, where accelerations for the four vehicles are plotted versus time (compare this to figure 2.10). The acceleration overshoot for the follower vehicles can be as high as 6 mph/second in this case. It is important to note that these accelerations only occur for a short period of time, so that the vehicles are still able to maintain safe headways between themselves and the vehicles in front of them.

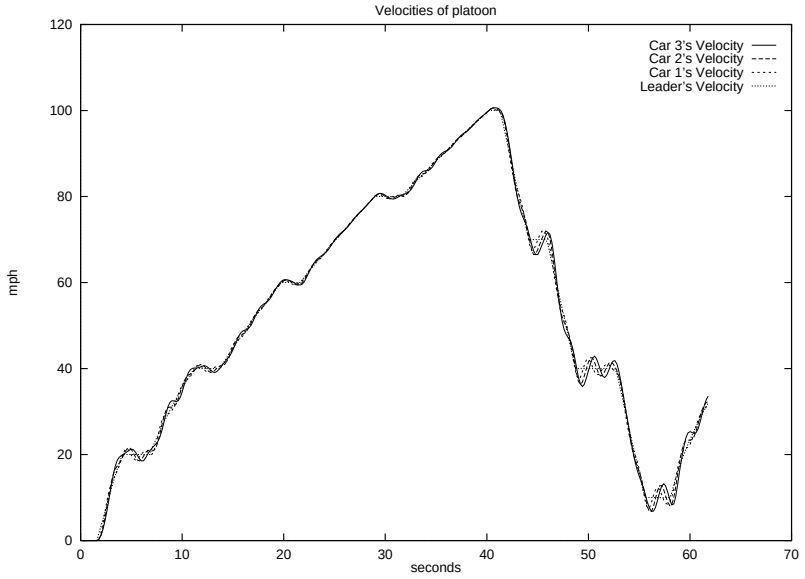

Figure 2.13. Velocity profiles for a four vehicle platoon under perturbed CICC control.

The corresponding emissions for these velocity/acceleration profiles are shown in figure 2.15 for CO, and 2.16 for NO_x. The acceleration spikes of the follower vehicles shown in figure 2.14 lead to high power demands on the engines, which are severe enough to drive the emissions control system into power enrichment mode. During these power enrichment events, the amount of CO produced is nearly 60 times as much as during normal controlled conditions. These CO (and HC) spikes occur more readily when the vehicle is at higher speed since the demanded acceleration values will easily exceed the power threshold required for an enrichment event. The NO_x emissions shown in figure 2.16 do not exhibit the same spike response, but they are roughly linear in response to acceleration.

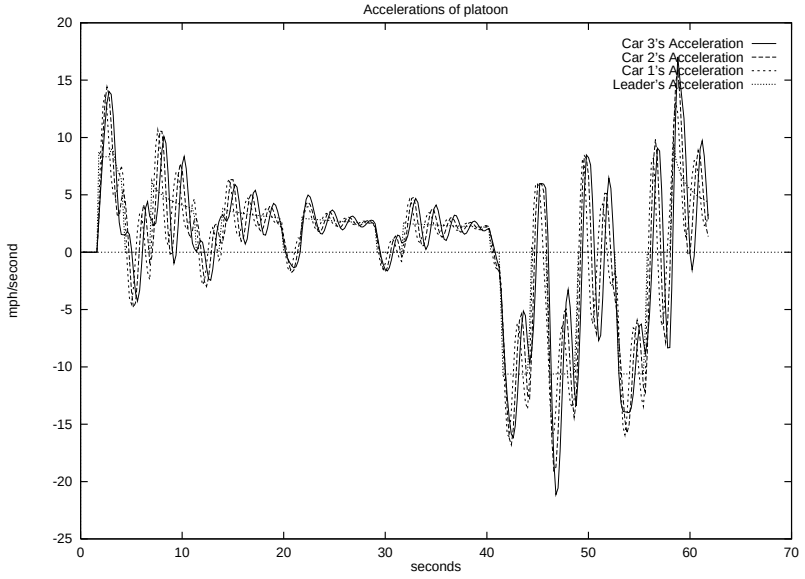

Figure 2.14. Acceleration profiles for a four vehicle platoon under perturbed CICC control.

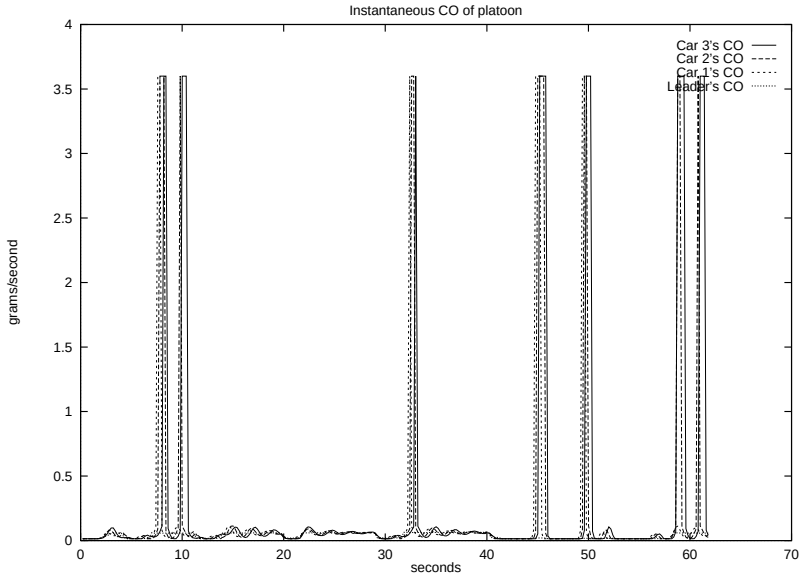

Figure 2.15. CO emissions versus time for a four vehicle platoon under perturbed CICC control.

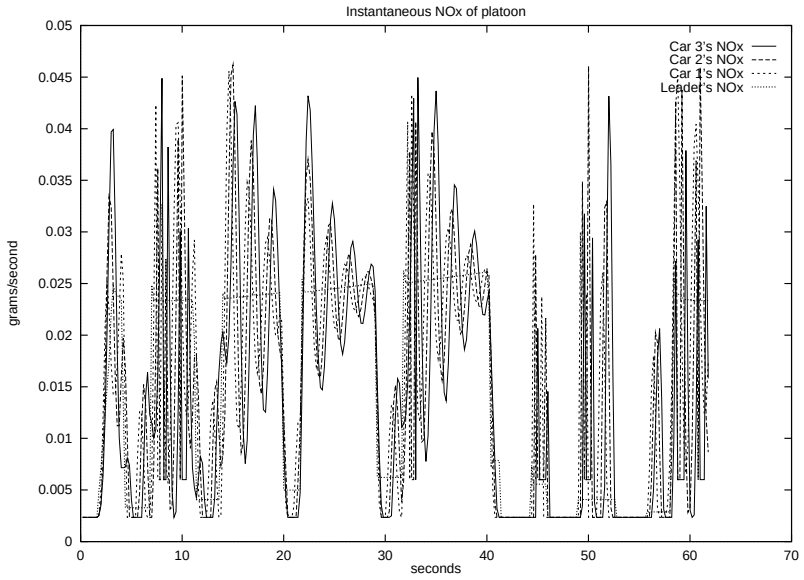

Figure 2.16. NO_x emissions versus time for a four vehicle platoon under perturbed CICC control.

An accumulation of CO emissions during the driving cycle for both perturbed and non-perturbed control is shown in figure 2.17. The perturbed control case is shown to exceed the non-perturbed case with significant increases during the enrichment events. Similarly, accumulative NO_x emissions are shown for both cases in figure 2.18. Because NO_x does not have the same response during enrichment events, the emissions for both cases are roughly the same.

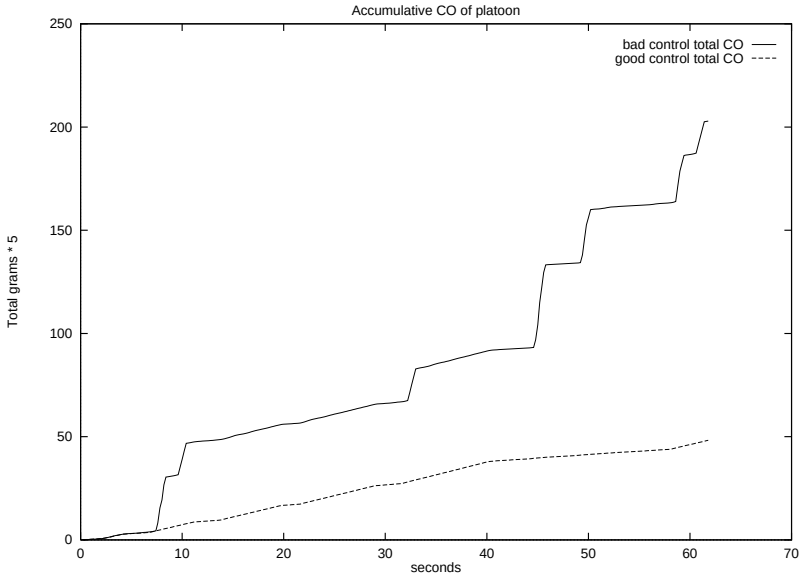

Figure 2.17. Accumulative CO emissions for both perturbed and non-perturbed control cases.

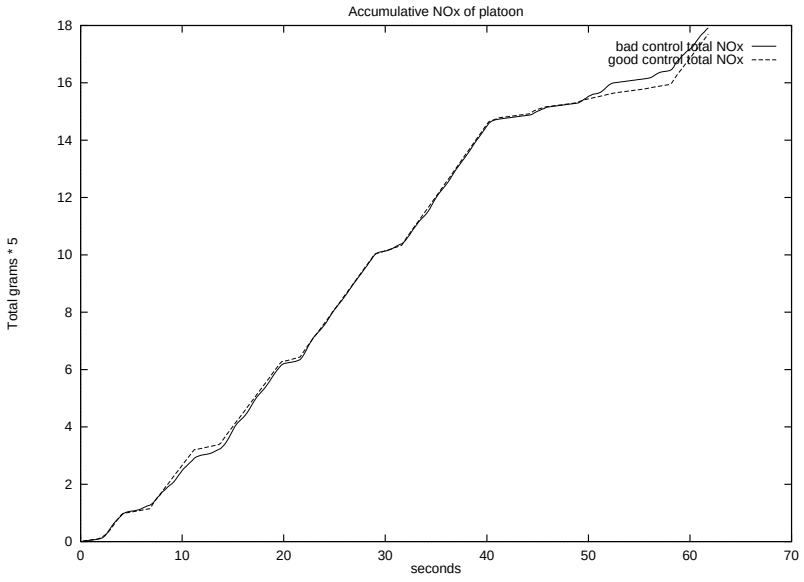

Figure 2.18. Accumulative NO_x emissions for both perturbed and non-perturbed control cases.

2.5.2 CICC vs. AICC comparison

In a similar fashion to the previous CICC case, an AICC control algorithm (Ioannou et al. 1992) was tested in the simulation experiments, using a wide range of driving cycles. The velocity and acceleration profiles of the leader vehicle and 3 follower vehicles for the same example driving cycle are shown in figures 2.19 and 2.20 respectively. It is apparent that there is little difference between these and the CICC case portrayed in figures 2.9 and 2.10, except for a more noticeable lag that occurs with the following vehicles. This lag is more prominent since information is not passed from the leader to the followers as in the CICC case. Each follower must wait for the previous vehicle to react its previous vehicle, thus the time lag propagates down the platoon. Similarly to the CICC case, there is little overshoot in the accelerations. The amount of CO and NO_x emissions, shown in figures 2.21 and 2.22, also vary little from amounts shown in the CICC case (figures 2.11 and 2.12).

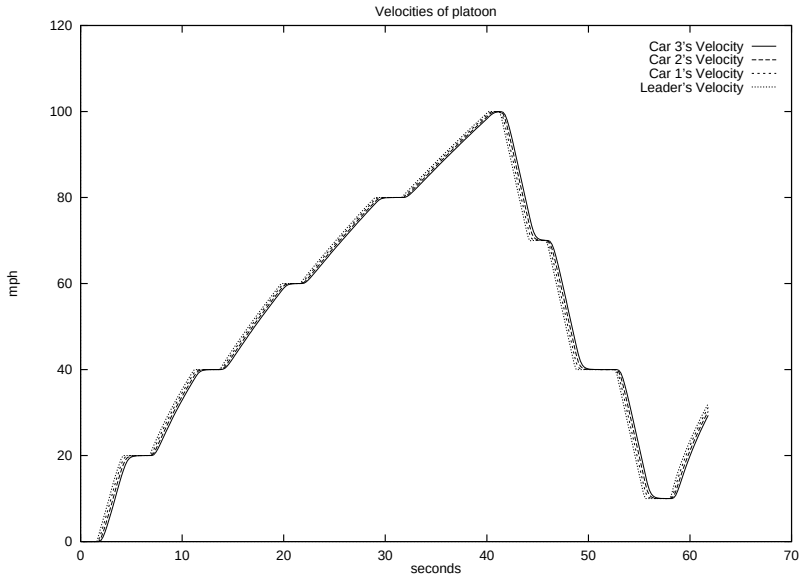

Figure 2.19. Velocity profiles for a four vehicle platoon under AICC control.

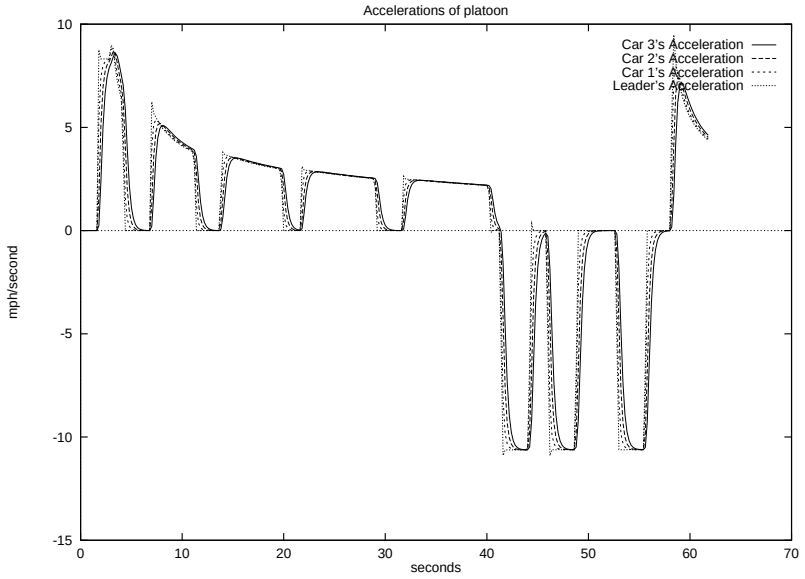

Figure 2.20. Acceleration profiles for a four vehicle platoon under AICC control.

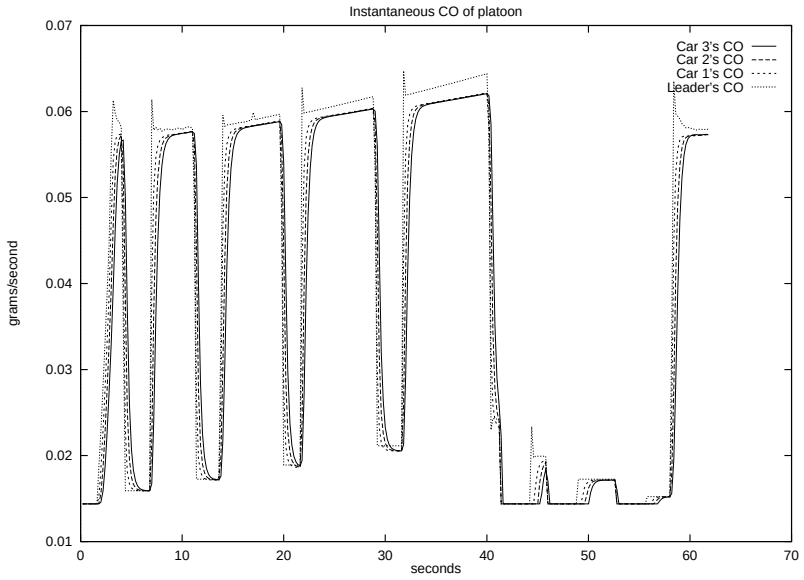

Figure 2.21. CO emissions versus time for a four vehicle platoon under AICC control.

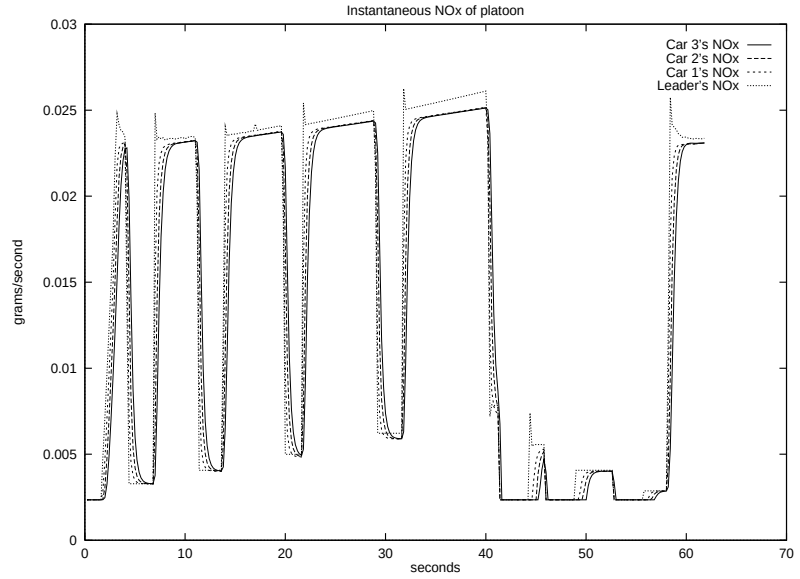

Figure 2.22. NO_x emissions versus time for a four vehicle platoon under AICC control.

3 Vehicle Emissions due to Ramp Metering

It has been suggested in recent years that ramp metering may be counter-productive from an air quality point of view. Many view ramp metering as a traffic control technique which shifts congestion off of the freeway and on to the surface streets, while at the same time inducing more demanding accelerations on the freeway on-ramps. In order to analyze the impact of ramp metering on air quality, we have identified three primary sources of influence that ramp metering may have directly on vehicle emissions:

Freeway traffic smoothing—The primary intent of ramp metering is to smooth the traffic flow on the freeway mainline and reduce overall delay for freeway travelers. By limiting the input volume to the freeway, overall freeway speeds can be increased. Further, by spacing out merging vehicles from the freeway on-ramps, the probability of acceptable gaps in the freeway traffic is much higher, causing fewer perturbations to the traffic flow. The overall traffic flow is smoother and faster, resulting in lower emissions.

Ramp, surface street congestion—When vehicles on a ramp are metered, congestion can occur on the ramp and associated surface streets under heavy traffic conditions. This congestion is characterized by slow, stop-and-go traffic conditions, leading to higher emissions produced by the vehicles waiting to get on the freeway.

Hard accelerations from the meters—When a vehicle finally reaches the ramp meter and eventually proceeds on to the freeway, it must accelerate rapidly to reach the freeway traffic speed. These accelerations put an enormous load on the engine and can result in relatively short bursts of high emissions.

Each one of these direct effects is being evaluated *independently* in this current year's work, and are described separately below. It is important to point out that ramp metering can also significantly reduce the number of freeway incidents (i.e., traffic accidents), thus improving freeway speeds, leading to lower emissions. We do not consider this and other indirect effects in this report.

3.1 MAINLINE TRAFFIC SMOOTHING

Ramp metering does not increase the capacity of the freeway, but rather protects it from break down by allowing only one vehicle at a time to enter the freeway. When a long string of unmetered traffic packed closely together merges from a ramp, typically there are insufficient

gaps in the freeway flow to accommodate all of them. This causes vehicles to slow down and possibly switch lanes, causing disturbances to freeway traffic. By eliminating these disturbances, the overall traffic flow can be smoother and faster, resulting in lower emissions.

A review of various ramp metering studies conducted in different parts of the US (e.g., Denver, Detroit, Portland, Seattle and Los Angeles) indicates a wide range of reductions in travel times and increases in speeds on the freeways (Robinson et al. 1989) . For example, in the operational system in Minneapolis-St. Paul, evaluations have shown that average freeway speeds increased from 55 to 74 km/hr (34 to 46 mile/hr, 35% improvement) (Robinson et al. 1989) .

In the paper (Corcoran et al. 1989) , ramp metering effects in Denver area were described. Before and after studies at one of the five freeway demonstration project locations indicated a 58% increase in travel speed (from 53 to 84 km/hr) during the AM peak period. Subsequently, the study area has been further expanded to 26 locations and similar results were observed.

The study (Robinson et al. 1989) summarized the ramp metering application in several U.S. cities. For example in Portland, Oregon there was a 156% increase in average speed on the north-bound PM peak hour traffic along I-5. Between 1981 and 1987, travel times decreased by 48% due to ramp metering implementation in Seattle, Washington. Similarly, in Detroit, Michigan and Austin, Texas freeway speeds increased by 8% and 60% respectively.

There have also been several simulation model implementations to analyze the effects of ramp metering. For example, Al Kadri developed a discrete, stochastic, mesoscopic simulation model within the framework of contextual systems approach for freeway ramp metering control (AlKadri 1991) . Further, Hamad utilized the Integrated Traffic Simulation (INTRAS) model to study various strategies of metering flow onto the freeway as well as between the freeways to evaluate the benefits of such strategies (Hamad 1987) . In all simulation experiments described in the literature with the exception of Denver study, there has not been a direct analysis of the effects on vehicle emissions.

Because current emission models such as CARB’s EMFAC and EPA’s MOBILE are based on average emissions over extended driving cycles and are insensitive to localized variations in speed and acceleration, they can not be efficiently combined with microscale traffic simulation models that are capable of simulating ramp metering. However, by using a modal emission model such as the approach described in appendix A, the impact on vehicle emissions can be evaluated.

In order to estimate the mainline speed increase due to ramp metering and its effect on emissions, several simulation experiments using the model FRESIM (summarized in the next section) were performed. These simulation experiments were carried out with the following two objectives in mind:

1) to confirm the previously established relationship between ramp volumes and mainline freeway speeds in case of non-metered ramps;

2) to study the impact of varying ramp meter cycle times on mainline freeway speeds for different ramp volumes.

Based on the measured speed increase, we then predict the overall emissions benefit using results of our emissions modeling.

3.1.1 FRESIM Summary

FRESIM is a microscale freeway simulation model in which each vehicle is modeled as a separate entity. The behavior of each vehicle is modeled in detail through the interaction with the surrounding environment which includes the freeway geometry and other vehicles. FRESIM is an improved model over its predecessor INTRAS. FRESIM can simulate a wide range of freeway geometrics which include one to five lane freeway mainlines with one to three lane ramps and interfreeway connectors, variations in grade, different radii of curvature, lane additions and lane drops anywhere on the freeway, freeway blockage incidents, and auxiliary lanes (lanes used to merge on and off freeway) (Halati et al. 1991) . It provides realistic simulation of operational features such as a comprehensive lane-changing model, clock time and traffic responsive ramp metering, comprehensive representation of the freeway surveillance system, representation of six different vehicle types including heavy vehicle truck movement, and can simulate ten different driver types ranging from timid to aggressive drivers. FRESIM also allows the user input of emission values for a speed/acceleration matrix (but not grade).

3.1.2 Simulation Setup

A two lane freeway segment with an on-ramp consisting of a single lane and a 152.4 meters (500 feet) merge section is considered for this simulation experiment, as shown in figure 3.1. A vehicle free flow speed of 96.5 km/hr (60 mi/hr) is set in the simulation, and only one type of vehicle (i.e., passenger vehicle) is considered in the simulated traffic flow. As before, FRESIM's acceleration/velocity vehicle performance table and emissions output was calibrated to a 1991

Ford Taurus. Each lane in the mainline traffic flow was set to carry a maximum flow of 2200 vehicles per hour. The simulation run time was set for 20 minutes.

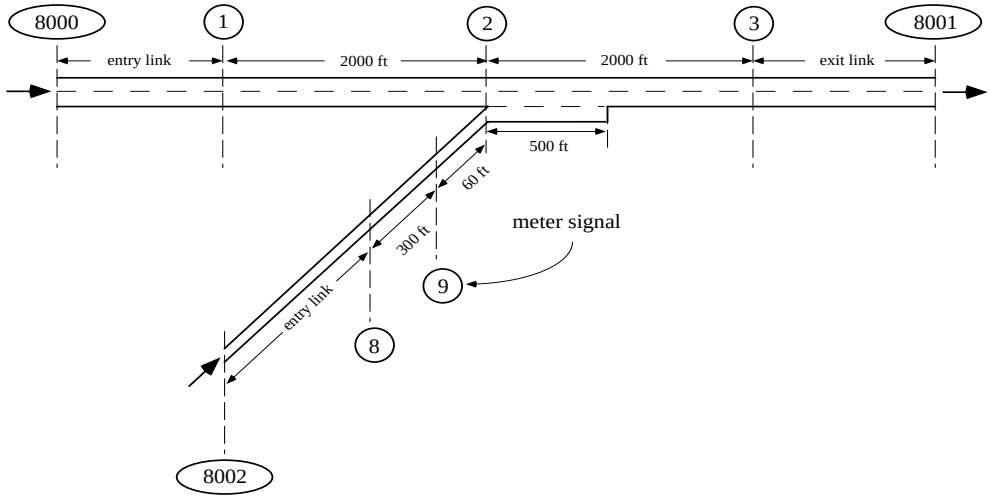

Figure 3.1. Freeway geometry for FRESIM ramp meter experiment (not to scale).

3.1.3 Mainline Speed Reduction due to High Ramp Volumes

A series of simulation runs was conducted to identify the relationship between non-metered ramp volumes and the corresponding mainline freeway speeds. Ramp volumes were varied from zero to 1200 vehicles/hour in increments of 200, while the upstream traffic volume remained at the constant 2200 vehicles per lane per hour. The corresponding mainline freeway speeds (average of speeds on links 1-2 and 2-3) were measured and plotted in figure 3.2.

Figure 3.2 confirms the fact that as ramp volumes increase, mainline freeway speeds drop significantly. However, a close look at the plot also reveals that the drop in speeds is more dramatic for lower ramp volumes (up to approximately 600 vehicles/hour-lane) when compared to higher volumes. The drop in the mainline freeway speeds is nearly 40% for ramp volumes of 600 vehicles/hour-lane from the 97 km/hr free speed. There is only a 24% drop between ramp volumes of 600 to 1200 vehicles/hour-lane. Overall, the freeway speeds fell approximately 54% from their free speed of 97 km/hr for a ramp volume of 1200 vehicles/hour-lane. More testing should be done using different ramp/freeway geometrics consisting of a larger number of lanes and different volumes on the freeway.

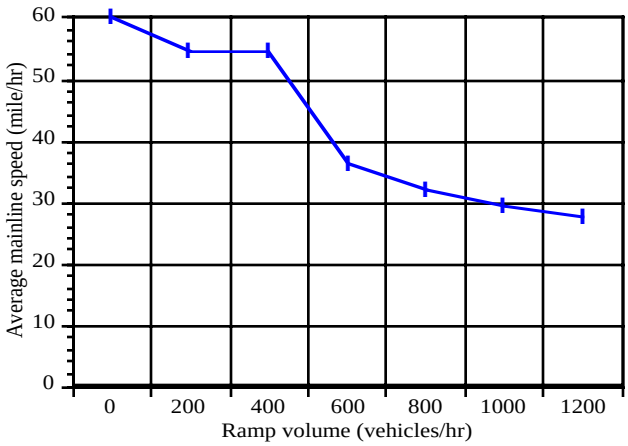

Figure 3.2. Average mainline freeway speed versus traffic volume on a non-metered ramp.

3.1.4 Mainline Speed Increase from Ramp Metering

As mentioned previously, freeway ramp control systems are used to control the flow of vehicles onto the freeway and thereby maintain freeway operations at an acceptable level of service. There are basically two types of ramp metering available: fixed time and traffic responsive. Fixed time control is obtained by presetting the metering rates in accordance with time of the day based on historical data such as volume from the mainline and the ramps. Traffic responsive control is obtained by using real time volume, speed, and density data collected from vehicle detectors on the ramps and mainline.

Four different types of metering strategies can be implemented in FRESIM. They are 1) clock time ramp metering; 2) demand/capacity metering; 3) speed control metering, and 4) gap acceptance merge control metering. Card type 37 is used to code ramp metering in FRESIM. Depending upon the number coded (1, 2, 3, or 4) in the second entry (column 8) of this card, one of the four control strategies can be implemented. If '1' is coded in column 8, metering headway in seconds for clock time metering is specified in the fourth entry (columns 13-16). In case of demand/capacity metering (specified by coding '2' in the second entry), capacity of the freeway in vehicles per hour is entered in the fifth field (columns 17-20). The user must also specify the detectors on the link that will provide input to the metering algorithm using the metering detector specification card (card type 38) and the surveillance card (card type 28). If speed control metering strategy is selected by coding '3' in entry 2, then the first speed threshold is entered in entry 6 (columns 21-24). If the speed measured by the detector is below the speed threshold specified in this entry, the metering signal is set to the metering rate specified in entry 7 (columns 25-28). Gap acceptance merge control metering can be selected by coding '4' in entry 2. When this strategy is selected, the minimum acceptable gap, in tenths of a second, is specified

in entry 12 (columns 45-48). Ramp vehicles are released by the control signal to merge smoothly in gaps in this type of ramp control. Gaps are expressed in units of time and detected in the outside freeway lane. However, in our current simulation, only the first strategy i.e., clock time ramp metering, is implemented for testing various scenarios.

Simulation experiments were carried out using the same freeway/ramp geometry shown in figure 3.1. Again, upstream traffic volume remained at the constant 2200 vehicles per lane per hour and mainline traffic speeds were measured. Using the clock time ramp metering control strategy in FRESIM, different cycle lengths were tested at various ramp volumes. Figure 3.3 illustrates the relationship between various cycle times and average mainline freeway speeds for one particular ramp volume, i.e., 1400 vehicles/hour. Ramp meter cycle times were varied from 1 second to 8 seconds as shown in the plot. A close look at the plot reveals that mainline freeway speeds increased significantly from 25.4 mi/hr (40.8 km/hr) for zero second cycle length (i.e., no ramp metering) up to 52.27 mi/hr (84.1 km/hr) for a six second cycle length (more than doubled). For cycle lengths greater than 6 seconds, the speed increase was less dramatic (52.27 mi/hr (84.1 km/hr) at 6 seconds to 54.35 mi/hr (87.5 km/hr) at 8 seconds).

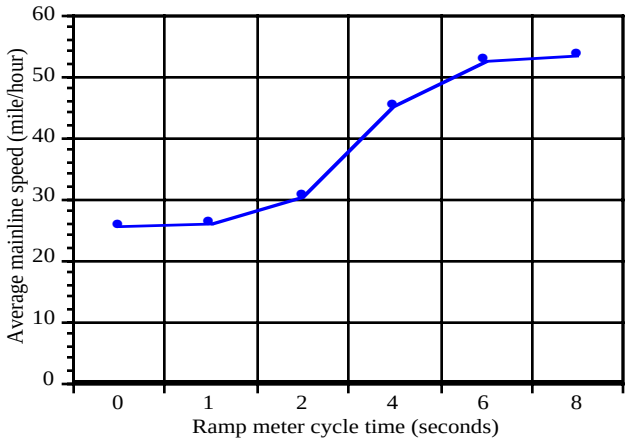

Figure 3.3. Average mainline freeway speed versus ramp meter cycle time for 1400 veh/hr ramp volume.

Based on the modal emissions model calibrated for the Ford Taurus, we have also acquired emissions as a function of meter cycle time. Figure 3.4 shows total link emissions for carbon monoxide. Similarly, figures 3.5 and 3.6 illustrate the dependence of hydrocarbons and oxides of nitrogen on meter cycle time. These emission values are given as grams per second per mile on the freeway link.

It can be seen that the emissions go up slightly for ramp meter cycle times of one and two seconds. This is due to the fact that ramp metering at this rate does not limit the traffic volume on the ramp (a one second interval corresponds to a max flow rate of 3600 vehicles/hour-lane, two

seconds corresponds to 1800 vehicles/hour-lane; these values are above the 1400 assigned volume). However, by spacing out the vehicles entering the mainline flow, the traffic turbulence is less, and the average vehicle speed is higher. In the model FRESIM, the amount of emissions is maximum around the average speeds of 30 to 45 mi/hr (48 to 72 km/hr), due to larger variations in vehicle velocity profiles (i.e., stop-and-go traffic). Thus, by first improving average traffic speeds slightly, emissions will reach a peak value, before falling off at higher average speeds.

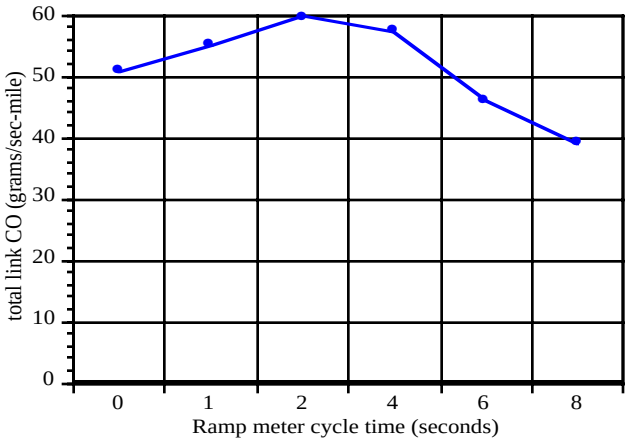

Figure 3.4. CO emissions rate per mile versus ramp meter cycle time.

3.2 RAMP QUEUING

While managing traffic congestion, ramp metering shifts the congestion off the freeway mainline, placing it on the freeway entrance ramps and associated surface streets. Ramp metering gives priority to mainline traffic at the expense of those entering the freeway. This often leads to significant backups behind the meters as well as on local surface streets if meters are not properly timed. In general, most of the ramp metering systems are implemented only during peak traffic periods.

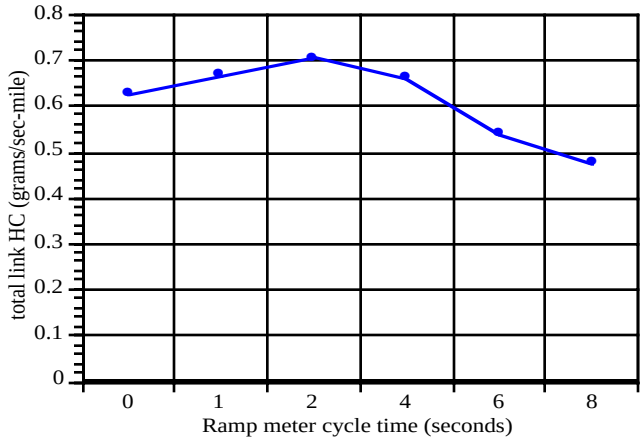

Figure 3.5. HC emissions rate per mile versus ramp meter cycle time.

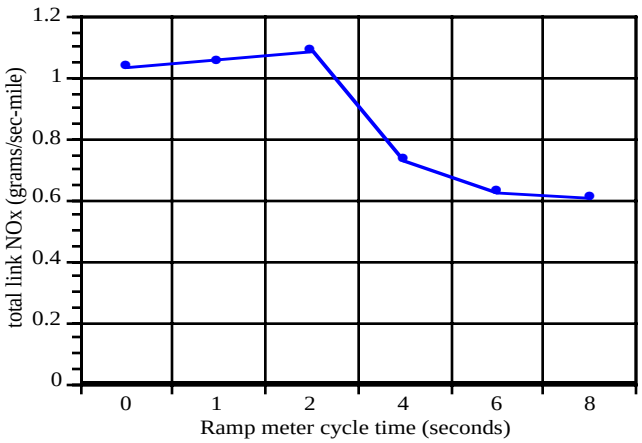

Figure 3.6. NO_x emissions rate per mile versus ramp meter cycle time.

In order to evaluate vehicle emissions caused by this congestion shift, we have performed a set of simulation experiments that analyze vehicle queuing on freeway ramps. In this preliminary evaluation, we analyzed only the congestion that forms on the freeway on-ramp itself, ignoring the congestion that spills onto the surface streets.

The simulation is carried out using a simulation program capable of modeling vehicles individually, described in (Barth et al. 1993). The microscale simulation model is very similar to the platoon simulator described in detail in chapter two, which models individual vehicle dynamics. The primary difference between the two is that instead of generating platoons and modeling automated vehicle control algorithms, vehicles are generated individually and manual car-following logic is employed.

We considered the same road geometry as shown in figure 3.1. The length of the ramp is 500 ft (152 meters) and near the entrance of the mainline freeway, there is a ramp meter with variable cycle times. We are mainly concerned with the amount of emissions and wait time associated with the ramp meter cycle times. It is assumed that for each green interval of the meter, only one vehicle can proceed (green time is approximately one second). The meter cycle time is then measured as the total duration between green times (i.e., red time + green time).

In all of the simulation experiments, the entire length of the on-ramp is loaded with vehicles. Vehicles are generated at the beginning of the ramp at the maximum generation rate that the on-ramp can handle, with the initial vehicle velocity matched to the average speed of the queue. Various experiments have been carried out with different meter cycle times. The density of vehicles, given in number of vehicles per foot, is shown as a function of cycle time in figure 3.7. It is apparent that as the cycle time increases, so does the density. A polynomial fit of the order

three was made to the measured data and is also shown in the figure. The error bars associated with the data points correspond to the standard deviation in measurements for each cycle time.

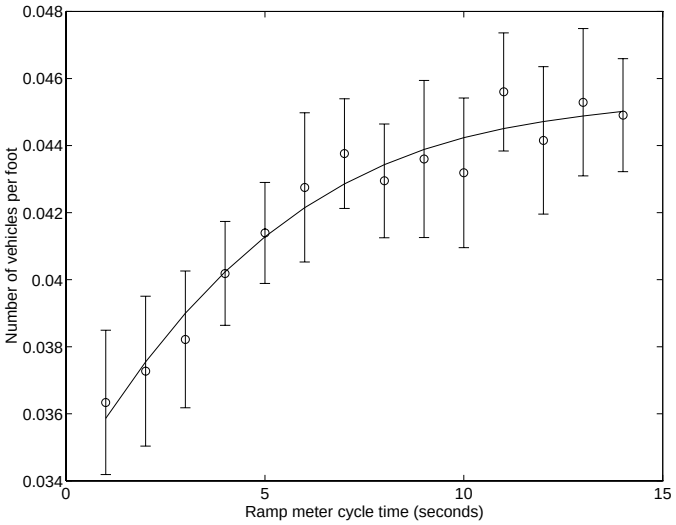

Figure 3.7. Vehicle density versus ramp meter cycle time.

Similarly, the relationship between average queue velocity and ramp meter cycle time is shown in figure 3.8. Since longer cycle times generate more vehicles on the on-ramp, the average velocity of the entire queue is decreased. As before, the error bars associated with the data points correspond to the standard deviation in measurements for each cycle time, and a polynomial of order three is also shown in the graph.

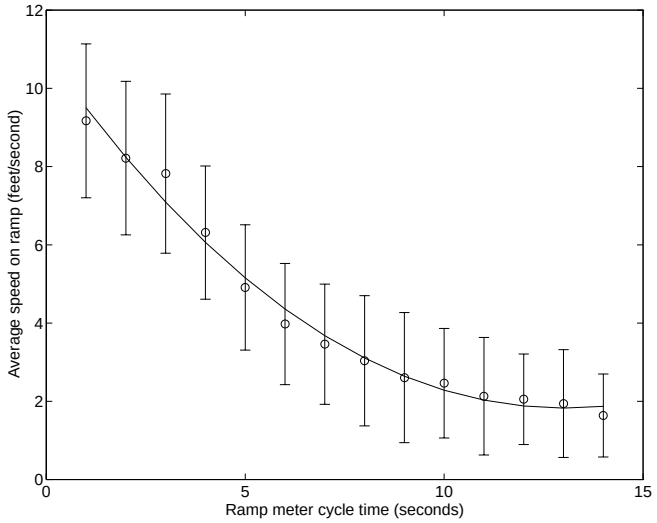

Figure 3.8. Average vehicle speed on ramp versus ramp meter cycle time.

Using the modal emissions model with the ramp queuing simulations, we are able to predict CO, HC, and NO_x emissions for different steady-state ramp cycle times. These results are shown in figure 3.9. It is apparent that with shorter meter cycle times, emissions are generally greater due to higher fluctuations in speed (i.e., greater number and larger magnitudes of accelerations, decelerations). With a longer red interval time, the number of vehicles on the ramp is high and the vehicles on the ramp are very passive due to longer stop times.

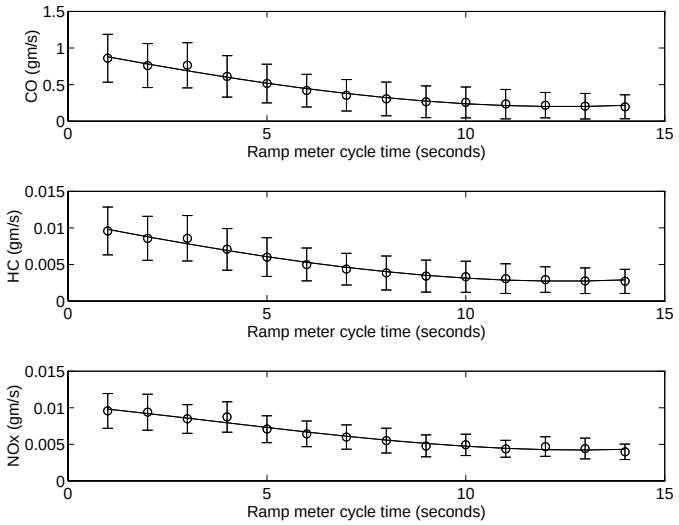

Figure 3.9. Emissions versus ramp meter cycle time.

Finally, the time an individual vehicle has to spend on the ramp increases when the red time is longer. This is shown in figure 3.10, where data was taken for several meter cycle times. As before, a polynomial fit is also shown and the error bars correspond to the standard deviation in the multiple samples around each data point. At higher wait times, the standard deviation of the times also increases.

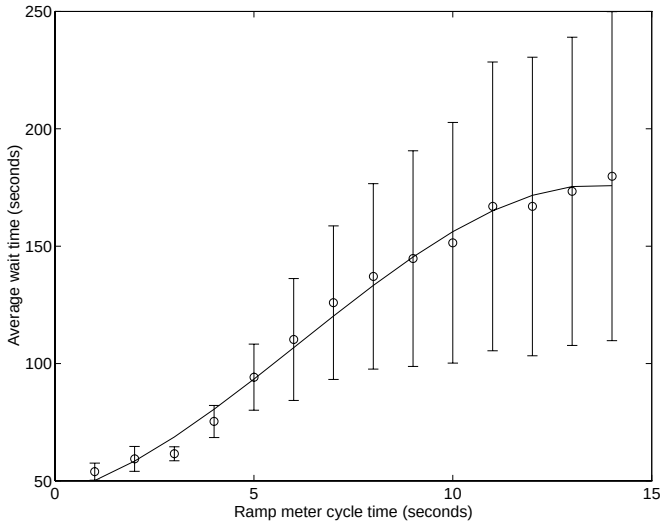

Figure 3.10. Average wait time versus ramp meter cycle time.

3.3 HARD RAMP ACCELERATIONS

The third, and possibly most overlooked impact ramp metering may have on vehicle emissions is the inducement of hard accelerations from the ramp meter to the freeway merge points. Because ramp meters effectively shorten the distance a vehicle has to accelerate up to freeway speeds, greater loads are placed on the vehicle engine, resulting in higher emissions. As described in appendix A, under heavy load conditions, a modern closed-loop emission controlled vehicle will enter a "power enrichment" mode under high engine load conditions. When in the power enrichment mode, the air-fuel ratio is commanded rich in order to protect the catalytic converter from excessive heat and to obtain a greater boost in power. During this enrichment mode, vehicle emissions are significantly higher (three orders of magnitude) (Meyer et al. 1992; Cadle et al. 1993; Kelly et al. 1993) .

We have developed a simulation model that predicts velocity and acceleration profiles for vehicles accelerating between constrained speeds and distances, when engine power is kept constant. This model has been combined with the modal emissions model described in appendix A, which takes into account the phenomenon of power enrichment. With such a model, it is possible to predict emissions produced during various cases of ramp accelerations.

Given initial starting and final speeds, road grade, and distance to accelerate, the model iterates over several constant engine power levels to determine whether the vehicle can obtain the final velocity in the prescribed distance. The main assumption of this method is that the engine power level remains constant throughout the entire acceleration. This assumption is roughly equivalent

to having a driver determine the required throttle position at the start of the acceleration (knowing the distance and grade), and keeping the throttle position constant throughout the entire acceleration. For each power level, the model updates the acceleration of the vehicle every second using equations of vehicle dynamics. Also updated are the vehicle's velocity and position. If the vehicle reaches the end of the prescribed distance and is not at the required speed, a higher engine power constant is chosen, and the process repeats until a successful acceleration is achieved. The emissions are then calculated for that engine power level for the duration of the acceleration.

This simulation model has been used to evaluate a small sample of freeway on-ramps in Southern California and it was found that some ramps are so short and steep that they produce upwards of 200 times as much CO emissions as that produced at freeflow freeway speeds, based on the same power demand modal emissions model used before.

The effect of grade is significant, as shown in figure 3.11. The simulation model was run on a fictional ramp of a constant length of 1393 ft (424 meters) and varying grade. The initial starting speed was set to 10 mi/hr (16 km/hr) and the final speed to 55 mi/hr (88.5 km/hr). It is apparent that there is a dramatic change in emissions when we plot the relative emissions versus the ramp grade as shown in figure 3.11 (the emissions values have been normalized to emissions for a 0% grade). The sharp increase in CO and HC emissions occurs when the vehicle goes into a power enrichment mode, while NO_x values decrease.

A typical set of velocity and acceleration curves are plotted versus time in figures 3.12 and 3.13. These curves correspond to the zero grade case for an acceleration from 10 to 55 mi/hr (16 to 88 km/hr). Note that the instantaneous acceleration of the vehicle steadily decreases when the engine power demand is kept constant.

The constant power demand assumption will generate accelerations that may not truly characterize actual on-ramp accelerations. In order to determine actual velocity and acceleration profiles on ramps, the California Air Resources Board and Caltrans have sponsored a study of freeway on-ramp accelerations, performed by researchers at California State Polytechnical University, San Lusi Obispo (Sullivan et al. 1993). We have recently obtained the final report and data and are attempting to merge the profiles and our emissions model.

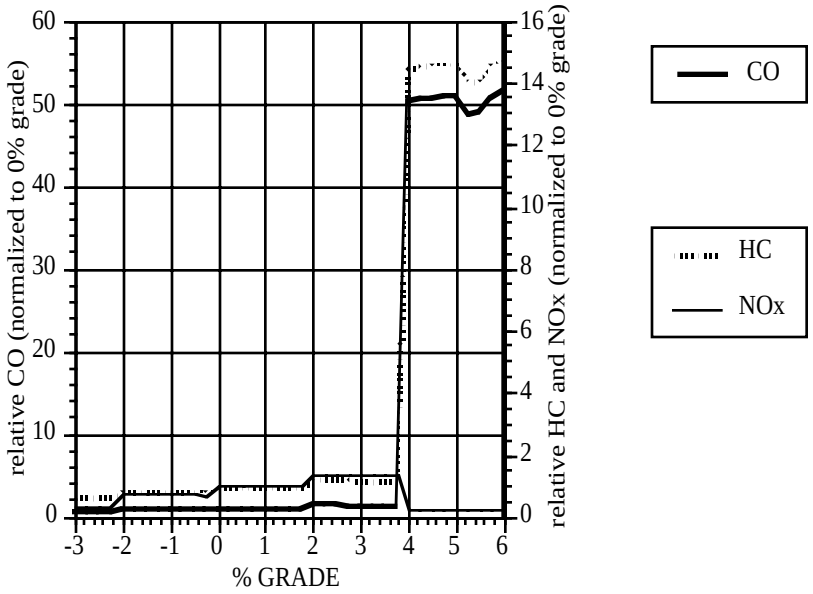

Figure 3.11. CO, HC and NO_x emissions for a constant length (424 meters, 1393 ft) and varying grade.

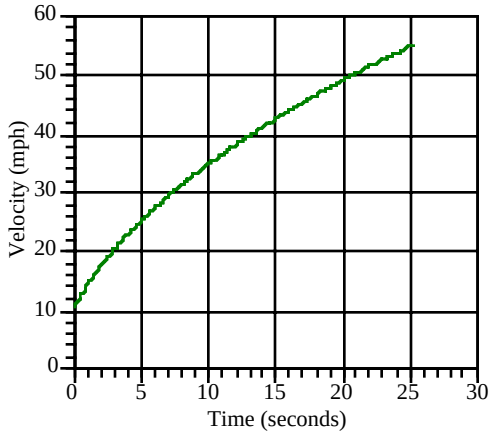

Figure 3.12. Velocity vs. time for zero grade, accelerating from 10 to 55 mi/hr (16 to 88 km/hr).

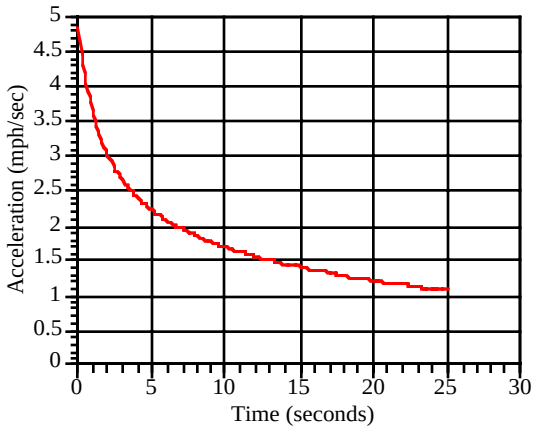

Figure 3.13. Acceleration vs. time for zero grade, accelerating from 10 to 55 mi/hr (16 to 88 km/hr).

This study has created a data set describing vehicle speeds and accelerations along a selected sample of freeway on-ramps having a variety of physical and operational characteristics. Speed and acceleration data were obtained for four different Caltrans districts and the sample was split between ramps with and without ramp metering. In addition to the acceleration and velocity data, mainline traffic conditions were also recorded. The velocity and acceleration profiles were recorded for approximately 100 different vehicles on each ramp. The measurements were made using a video camera which observed the starting point of the ramp (or meter location) and the final merge point on the freeway.

For each ramp, average speed and acceleration profiles were calculated. In addition, due to the large variations in different vehicle acceleration and velocity profiles on the same ramp (under similar traffic conditions), the profiles were ordered based on a summation of instantaneous power demand. Examples of the 15%tile, 50%tile, and 85%tile power ordering are given, representing passive drivers (15%tile), average drivers (50%tile), and aggressive drivers (85%tile). Three examples of these different velocity profiles on a sample ramp are shown in figure 3.14, and the corresponding acceleration profiles are shown in figure 3.15. This sample ramp (Ventura Fwy US 101 at Calabasas, Southbound) is 1300 feet long (396 meters), straight, and has a -6.30% grade. Each curve in these figures corresponds to a sample of the 15%tile, 50%tile, and 85%tile power ordering. It is apparent that there is a large amount of variation between these three sample velocity/acceleration profiles. The starting velocity in these examples varies from 16 to 27 mi/hr (26 to 43 km/hr) and the final velocities are around 45 to 50 mi/hr (72 to 80 km/hr).

A key difference between these velocities/accelerations and those that are predicted by our simulation model is that there is a considerable time lag (3-5 seconds) before peak acceleration is

achieved. This implies that in general, drivers ease the throttle forward over a few seconds rather than immediately stomp down on the pedal. It is apparent that after peak acceleration is achieved, the acceleration decays as speed increases, as is predicted by the simulation model. However, in these examples, the drivers tend to "correct" their acceleration near the end of the ramp in order to enter traffic. This phenomenon is not modeled in the simulation.

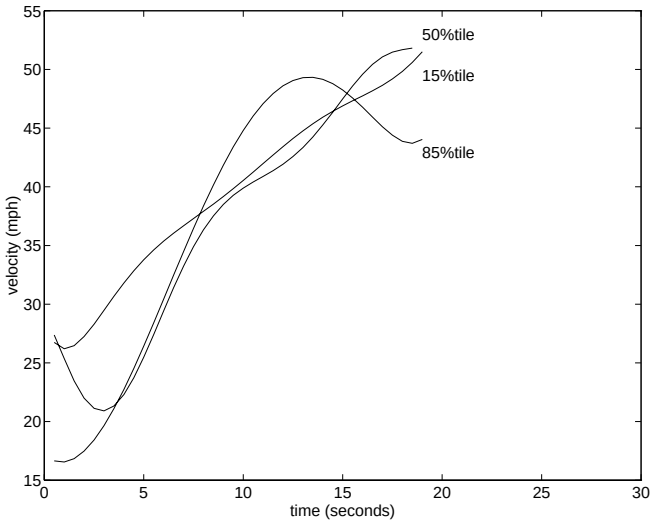

Figure 3.14. 15%tile, 50%tile, and 85%tile sample velocity profile for example ramp from CalPoly study (Sullivan et al. 1993) .

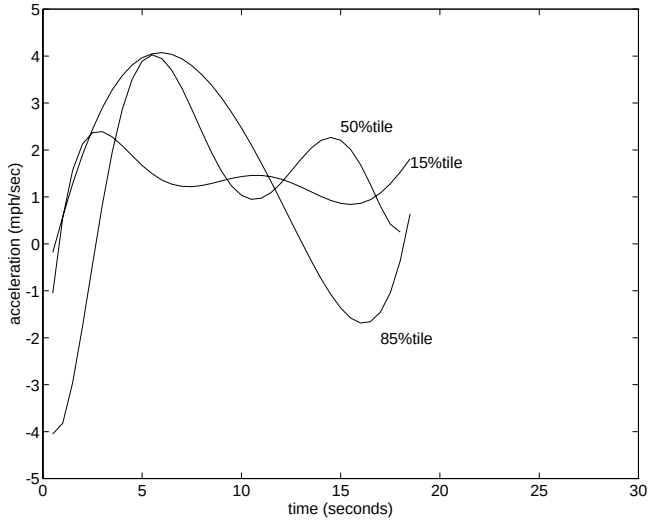

Figure 3.15. 15%tile, 50%tile, and 85%tile sample acceleration profile for example ramp from CalPoly study (Sullivan et al. 1993) .

The effective shortening of acceleration distance due to ramp metering has been analyzed in the CalPoly study. It concludes that although there are a variety of different acceleration profiles on the ramps, accelerations from ramp meters generally consist of higher power demand, at least

initially in the acceleration profile. The higher power demand will thus in turn produce higher emissions.

We plan to apply our modal emissions model to the CalPoly data in order to determine emissions variations corresponding to different ramp parameters. With further analysis, we will be able to see the emissions impact of aggressive versus passive drivers, the effect of ramp curvature, ramp metering versus non metering, etc.

4 Conclusions and Future Work

The continued research and development of ITS-related simulation models combined with modal emission models will allow us to improve our understanding of ITS vehicle activity and the associated emissions. The problems with current emission models along with a description of the first year project tasks is provided in chapter 1. Chapter 2 discusses work carried out in the area of platooning and some preliminary emission results related to different control algorithms. Finally, chapter 3 discusses the preliminary results of ramp metering and its effect on vehicle emissions. Overall conclusions and recommendations for future work are presented in this chapter.

4.1 AHS VEHICLE EMISSIONS CONCLUSIONS

Based on microscale simulation models and modal emissions data for a modern, closed-loop emission controlled vehicle, steady-state (i.e., constant velocity) emission rates have been estimated for both manual and automated lanes. An automated lane using platooning can improve the traffic flow by a factor of four, and at maximum flow values, the total emissions increase is by a factor of two (for the modeled Ford Taurus). If only half of the automated lane capacity is used, the traffic flow improves by a factor of two, and the associated emission rates are roughly the same as the full-capacity manual case. If the automated lane carries the same traffic volume as in the manual case, the emissions are reduced by a factor of two.

We are currently using our models to predict the emissions associated with stop-and-go traffic in the unstable traffic flow-density regions (based on the modeled Ford Taurus). If congestion is to be avoided, the traffic should be kept in the positive slope region of the flow-density curve (see figure 2.4). When in the positive slope region, interaction between vehicles in traffic is minimal, leading to smoother traffic flow. It can be seen that the extent of the positive slope region is much greater for the automated lane when compared to the manual lane. For the automated case, the network and link layer controllers in the AHS will attempt to keep traffic in the stable operating regime at all times.

This analysis assumed a constant platoon size of 20 vehicles, however, platoons will vary in length due to vehicles dynamically entering and leaving platoons as they travel from their specific origins to destinations. Shorter length platoons will lead to lower automated lane capacities and higher average vehicle emissions. Also, emissions associated with platoon maneuvers such as *splitting* and *merging* have not been analyzed here, but will be investigated in the second year of work. Automated platoon merging may induce significant emissions when velocities are high and merging gaps are small.

Emissions associated with velocity transients were also analyzed with the developed platoon simulator. For smooth accelerations, transient emissions should be minimal. However, for velocity transients that place heavy load on the vehicles' engine, the emission control systems of vehicles may go into a power enrichment mode, leading to significantly higher emissions. When designing the control components of an AHS, it is important to consider the emission effects of these velocity transients (if vehicles utilizing an AHS have emission control characteristics as those modeled here).

It is also important to point out that even a small amount of acceleration oscillation caused by some type of perturbation in the platooning control constants may lead to higher emissions. This is particularly true at high speeds when the power demand on the engine is already fairly high. A small amount of commanded acceleration can drive the vehicle into a power enrichment mode.

A comparison between CICC and AICC control algorithms showed that there is little difference in vehicle emissions when the platoon control is operating correctly.

Finally, it is important to point out that the emission rates used in this analysis were for a single vehicle. For current manual driving, the vehicle population is quite varied, and to more accurately predict total emissions, emission rates for different vehicle classes must be incorporated. For an automated scenario, however, the vehicle population will be somewhat more restricted. Vehicles that have automated platoon technology will tend to be newer passenger vehicles with closed-loop emission control systems, similar to the vehicle modeled here. It may be that by the time AHS technology is in place in our transportation systems, vehicle emission control technology will have improved to the point where the potential problems outlined in this report do not apply.

4.2 RAMP METERING EMISSIONS CONCLUSIONS

Vehicle emissions associated with ramp metering have been analyzed, with an emphasis of three sources of influence: 1) freeway traffic smoothing, 2) ramp and surface street congestion, and 3) hard accelerations for the meters.

As expected, simulation experiments have shown that the use of ramp metering increases the overall traffic speed on the mainline by restricting the ramp volume and by minimizing the disturbances caused by merging vehicles. The emissions associated with this mainline speed increase are at first detrimental since the traffic enters a state of greater stop-and-go, even though the average speed is higher. For longer ramp meter cycle times, the freeway speeds increase further, and the total emissions decrease due to lower traffic density and smoother flow.

Queues of vehicles on the on-ramps and their emissions have been studied using a simulation model. It was shown that the density of vehicles increases for longer ramp cycle times, and the average vehicle speed on the ramps decreases. However, it was shown that emissions tend to be higher for shorter ramp meter cycle times, primarily due to an increased stop-and-go effect.

Finally, we have developed a simulation model that predicts velocity and acceleration profiles for vehicles accelerating under constrained speeds and distances, using constant engine power. This was applied to freeway on-ramps, in particular, accelerating from a ramp meter to the merge point on the freeway. If the distance is short (and if the grade is steep), the engine power required may cause the vehicle to go into the power enrichment mode, causing high emissions.

The velocity and acceleration profiles produced from the simulation model did not mimic very well profiles that were measured in the field. The key difference is that there is a considerable time lag (3-5 seconds) before peak acceleration is achieved in the measured profiles. This may contribute positively towards emissions since the transition in power enrichment may be delayed. Further improvements must be made to the simulation model to provide better emission analyses.

We plan to apply our modal emissions model directly to the measured profiles to determine emission variations corresponding to different ramp parameters. With further analysis, we will be able to see such things as the emissions impact of aggressive versus passive drivers, the effect of ramp curvature, and ramp metering versus non-ramp metering. Also, it might be useful to study the possible effects of re-routing that may occur when drivers attempt to avoid ramp meters. Previously uncrowded intersections and arterials may experience increased traffic and delays due to drivers re-routing. Although this effect may be minor in some cases, it may be significant in others.

4.3 FUTURE WORK

In the first year of work, vehicle emissions associated with platooning have been studied. In order to evaluate the total emissions from an Automated Highway System, further modeling must be performed. An AHS will likely consist of multiple automated lanes for platooned vehicles and a transition lane for manually driven vehicles to enter the automated lanes (see, e.g., Varaiya et al. 1991).

Vehicles in a complete AHS scenario will also undergo maneuvers such as platoon merging, platoon splitting, and free agent (single vehicle platoon) lane changing (see, e.g., Hsu et al. 1991). Also, transitioning from a manual lane to an automated lane needs to be evaluated. In the second year of work, we plan to integrate our modal emission model with the PATH-developed AHS simu-

lator SmartPath (Eskafi et al. 1992; Hongola et al. 1993). SmartPath is capable of simulating multiple platoons and the above mentioned maneuvers. The modal emission modeling component will be implemented as a module in SmartPath's modular architecture.

After evaluating SmartPath in this first year, it has been determined that it will be necessary to make modifications to some of SmartPath's routines in order to correctly estimate vehicle emissions. In particular, the mathematical formation characterizing the physics of speed and acceleration must be modified so that the vehicles operate in a realistic fashion, with respect to acceleration motion.

When the modal emission module is completely integrated with SmartPath and vehicle accelerations are properly modeled, total emissions for different AHS scenarios can be determined. The AHS emissions will then be directly compared to emissions from a highway of manually driven vehicles. This can be done using FHWA's freeway simulation model FRESIM. Further, total vehicle emissions are being estimated for different levels of congestion using Caltrans' I-880 database, which includes global traffic parameters (i.e., average speed, density, flow) for a 45 day period on California's I-880 freeway. The database also contains velocity profiles from instrumented vehicle runs which can be registered with the global traffic parameters.

Another area that can be explored as future work is an analysis of the problems associated with the end-points of automation, i.e., the dumping of high flow rates onto off-ramps, arterials, and collectors. In effect, automation causes peak period compression, meaning that higher flow rates occur throughout the system. In some cases this could cause congestion on off-ramps, arterials, and collectors at automation egress points. The emissions associated with these cases should also be examined.

Also in this first year of work, three sources of emissions related to ramp metering have been identified. Each emissions source was then evaluated independently. Emissions reduction from freeway smoothing was determined using the simulation model FRESIM. An emissions increase due to ramp queuing was determined using a lane queuing simulation model. Finally, emissions due to hard accelerations from the meters was determined based on a constant engine power assumption under constraints of start and end velocities, ramp grade, and ramp length. In the second year of work, we will attempt to *integrate* all of these sources of emissions together, under varying conditions of ramp metering.

Also, there are several sources of uncertainty in the emission estimation processes described in this report. In the second year of work, these uncertainties will be identified and their impact on the results will be given.

Lastly, it is important to point out that the emission estimates made in this report are based on the modeling of a single, modern emission controlled vehicle. Additional programs are underway around the country to collect modal emissions data for a larger set of vehicles, which will result in more robust modal emission models. As these data become more available, they can easily be incorporated into the models used in this report and the accuracy of emission estimates associated with ITS will improve.

5 References

AlKadri, M. Y. 1991. Freeway control via ramp metering : development of a basic building block for an on-ramp, discrete, stochastic, mesoscopic, simulation model within a contextual systems approach. Ph.D. Dissertation. Portland State University.

Barth, M. and J. Norbeck. 1993. The Development of an Integrated Transportation/Emissions Model to Predict Mobile Source Emissions. Center for Environmental Research and Technology, University of California, Research Report #FR-93-001.

Butler, J. 1992. Instrumenting a Ford Aerostar Van with a Fourier-Transform Infra-Red Spectrometer. CRC-APRAC On-Road Vehicle Emissions Workshop. Los Angeles, CA.

Cadle, S. H., M. Carlock, et al. 1991. CRC-APRAC Vehicle Emissions Modeling Workshop Summary. Journal of Air and Waste Management Association 41: 817-820.

Cadle, S. H., R. A. Gorse, et al. 1993. Real-World Vehicle Emissions: A Summary of the Third Annual CRC-APRAC On-Road Vehicle Emissions Workshop. Journal of Air and Waste Management 43: 1084 - 1090.

California Air Resources Board (CARB). 1991. Presented material at the Seminar on Transportation Modeling for Emissions Analysis: Theory and Practice. Sacramento, CA.

Corcoran, L. J. and G. A. Hickman. 1989. Freeway Ramp Metering Effects in Denver. Institute of Transportation Engineers, 59th Annual Meeting. San Diego, CA, 513-517.

Eisinger, D. 1993. Preview of MOBILE. Proceedings of Transportation Modeling: Tips and Trip-Ups. San Mateo, CA.

Institute of Transportation Engineers. 1992. *Traffic Engineering Handbook*. Englewood Cliffs, New Jersey. Prentice Hall, Inc.

Eskafi, F., D. Khorramabadi, et al. 1992. SmartPath: an Automated Highway System Simulator. ITS-PATH Technical Report, UCB-ITS-PTM-92-3.

Federal Highways Administration (FHWA). 1986. TRANSYT-7F: Traffic Network Study Tool (Version 7F). Washington, DC. U.S. Department of Transportation.

Federal Highways Administration (FHWA). 1989. TRAF-NETSIM User's Manual. US Department of Transportation.

Federal Test Procedure (FTP). 1989. Code of Federal Regulations. Title 40. Parts 86-99 (portion of CFR which contains the Federal Test Procedure), Office of the Federal Register.

Gillespie, T. D. 1992. *Fundamentals of Vehicle Dynamics*. Warrendale, PA. Society for Automotive Engineers, Inc.

Halati, A., J. Torres, et al. 1991. FRESIM - Freeway Simulation Model. Transportation Research Board 70th Annual Meeting. Washington, DC, paper # 910202.

Hamad, A.-R. 1987. Evaluation of Ramp Metering Strategies at Local On-Ramps and Freeway-to-Freeway Interchanges Using Computer Simulation. Ph.D. Dissertation. Michigan State University.

Hongola, B., J. Tsao, et al. 1993. SmartPath Simulator - Version MOU62. ITS-PATH Research Report, UCB-ITS-PWP-93-8.

Hsu, A., F. Eskafi, et al. 1991. The Design of Platoon Maneuver Protocols for IVHS. California PATH Program, ITS, University of California, UCB-ITS-PRR-91-6.

Ioannou, P. A., C. C. Chien, et al. 1992. Autonomous Intelligent Cruise Control. Surface Transportation and the Information Age, Proceedings of the IVHS America 1992 Annual Meeting. Newport Beach, California, 97 - 112.

Institute of Transportation Engineers (ITE). 1990. IVHS special issue. ITE Journal 60 (11).

Karaaslan, U., P. Varaiya, et al. 1990. Two proposals to improve freeway traffic flow. California PATH Program, ITS, University of California, UCB-ITS-PRR-90-6.

Kelly, N. A. and P. J. Groblicki. 1993. Real-World Emissions from a Modern Production Vehicle Driven in Los Angeles. Journal of the Air & Waste Management Association 43: 1351-1357.

Maldonado, H. 1991. Methodology to Calculate Emission Factors for On-Road Motor Vehicles. California Air Resources Board Technical Report.

Maldonado, H. 1992. Supplement to Methodology to Calculate Emission Factors for On-Road Motor Vehicles July 1991. California Air Resources Board Technical Report.

May, A. D. 1990. *Traffic Flow Fundamentals*. Englewood Cliffs, New Jersey. Prentice-Hall.

McGurrin, M. and P. Wang. 1991. An Object-Oriented Traffic Simulation with IVHS Applications. 2nd SAE Vehicle Navigation and Information Systems Conference. Dearborn, MI, 551-561.

Meyer, M., D. LeBlanc, et al. 1992. A Study of Enrichment Activities in the Atlanta Road Network. Proceedings of an International Specialty Conference on Emission Inventory Issues. Durham, NC.

Pipes, L. A. 1953. An Operational Analysis of Traffic Dynamics. Journal of Applied Physics 24(3): 274-287.

Rao, B. S. Y. and P. Varaiya. 1994. Potential Benefits of Roadside Intelligence for Flow Control in an IVHS. Transportation Research Board, 73rd Annual Meeting. Washington, DC.

Robinson, J. and M. Doctor. 1989. Ramp Metering: Does It Really Work? Institute of Transportation Engineers 59th Annual Meeting. San Diego, CA, 503-508.

Rockwell International. 1992. Potential Payoffs from IVHS: A Framework for Analysis. California PATH Program, University of California, UCB-ITS-PRR-92-7.

South Coast Air Quality Management District (SCAQMD). 1993. Presented material at the National IVHS and Air Quality Workshop. Diamond Bar, California.

Sheikholeslam, S. E. 1991. Control of a Class of Interconnected Nonlinear Dynamic Systems: The Platoon Problem. Ph.D. Dissertation. University of California, Berkeley.

St. Denis, M. and A. M. Winer. 1993. Prediction of On-Road Emissions and Comparison of Modeled On-Road Emissions to Federal Test Procedure Emissions. Air and Waste Management Association's The Emission Inventory - Perception and Reality. Pasadena, CA.

Sullivan, E. C., N. Devadoss, et al. 1993. Vehicle Speeds and Accelerations Along On-Ramps: Inputs to Determine the Emissions Effects of Ramp Metering. Technical Report, Transportation Research Group, Applied Research and Development Facility, California Polytechnic State University, San Luis Obispo, CA.

Transportation Research Board (TRB). 1985. Highway Capacity Manual, Special Report 209. Washington, DC.

Van Aerde, M. 1992. INTEGRATION: A Model for Simulation Integrated Traffic Networks, User's Guide for Model Version 1.4 d. Transportation Systems Research Group, Department of Civil Engineering, Queens University, CANADA.

Varaiya, P. and S. Shladover. 1991. Sketch of an IVHS Systems Architecture. California PATH Program, ITS, University of California, UCB-ITS-PRR-91-3.

Warner, C. 1985. Spatial Transportation Modeling. Beverly Hills. Sage Publications.

Zabat, M., S. Frascaroli, et al. 1993. Drag Measurements on 2, 3, & 4 Car Platoons. Technical Report, Department of Aerospace Engineering, University of Southern California, CA.

Zhang, W.-B., S. Shladover, et al. 1994. A Functional Definition of Automated Highway Systems. California PATH Program, ITS, University of California, UCB-ITS-PRR-94-9.

Appendix A: Power Demand Modal Emission Model

Second-by-second emissions data that are registered with vehicle dynamic operation are often referred to as *modal emissions data*—emissions data that correspond to a vehicle's operating mode, e.g., acceleration, deceleration, steady state cruise, idle, etc. Using modal data in an emissions model is in sharp contrast to the current FTP-based emission inventory techniques, where emissions are collected in bags over long periods of time (on the order of 500 seconds), and then analyzed as a whole.

In the simulation models, we consider at the fundamental level a vehicle's acceleration performance not only in implementing realistic simulations, but also in determining emissions output. A vehicle's acceleration performance (in the longitudinal direction) is limited by the engine power and the traction limits on the drive wheels. The engine power is modeled in detail based on torque curves that vary with engine RPM (Gillespie 1992). Given the instantaneous power requirements placed on a vehicle (at the wheels) for it to move depends on three types of factors:

1) **Environmental factors:** e.g., mass density of air, temperature, road grade;

2) **Static vehicle parameters:** e.g., vehicle mass, rolling resistance coefficient, aerodynamic drag coefficient, cross sectional area;

3) **Dynamic vehicle parameters:** e.g., commanded acceleration, and velocity.

Given these parameters and referring to figure A1.1, the inertial power requirements (in kilowatts) are given as:

$$P_{inertial} = \frac{M}{1000} \cdot V \cdot \left(a + g \cdot \sin\theta\right) \qquad \text{(A1-1)}$$

where M is the vehicle mass (kg), V is the vehicle velocity (meters/second), a is the vehicle acceleration (meters/second^2), g is the gravitational constant (9.81 meters/second^2), and θ is the road grade angle. The power requirements due to the drag components are given as:

$$P_{drag} = \left(M \cdot g \cdot C_r + \frac{\rho}{2} \cdot V^2 \cdot A \cdot C_a \right) \cdot \frac{V}{1000} \qquad \text{(A1-2)}$$

where C_r is the rolling resistance coefficient, ρ is the mass density of air (1.225 kg/meter^3), A is the cross sectional area (meter^2), and C_a is the aerodynamic drag coefficient. Thus the total tractive power requirements placed on the vehicle (at the wheels) is given as:

$$P_{total} = P_{inertia} + P_{drag} \tag{A1-3}$$

To translate this tractive power requirement to demanded engine power requirements, the following approximate equation is used:

$$P_{engine} = \frac{P_{total} \cdot \omega_e \cdot r}{\eta_{tf} \cdot N_{tf} \cdot V} \tag{A1-4}$$

where ω_e is the engine speed (radians/second), r is the radius of the drive wheels (meters), N_{tf} is the numerical ratio of the transmission and final drive, and η_{tf} is the combined efficiency of the transmission and final drive. Note we are ignoring inertia in the powertrain. The numerical ratio of the transmission depends of course on which gear the vehicle is in. In the case of manual transmission, gear selection is determined by the driver. In the case of an automatic transmission, the vehicle uses an internal gear selection strategy that depends on the demanded engine power and possibly other related inputs such as engine/vehicle velocity. If the gear number is known, it is possible to approximate the engine velocity from vehicle velocity based on the gear ratio information. Also incorporated within the engine power demand function is the operation of accessories, such as air conditioning, that can place additional power demand on the engine.

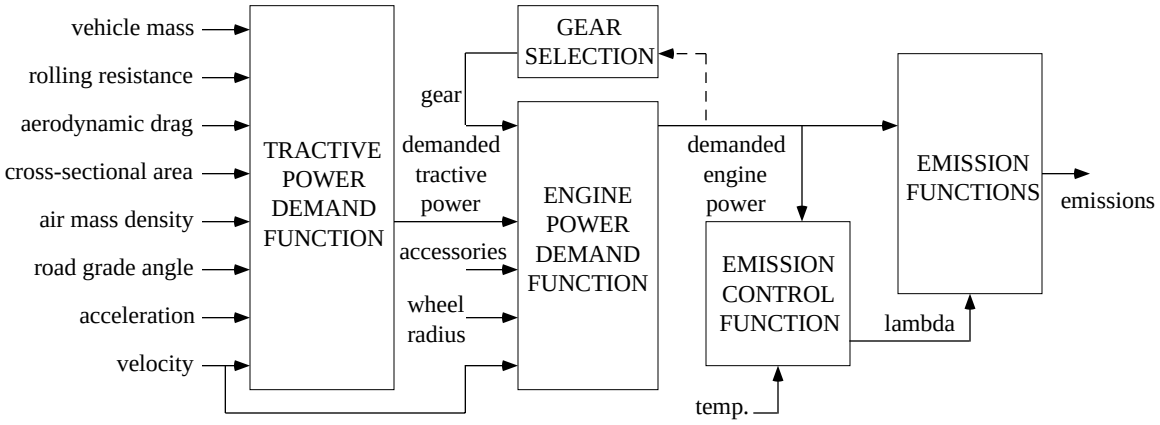

Figure A1.1. Load-based modal emissions modeling methodology.

One of the most important aspects of this load-based method for estimating emission output is modeling the vehicle's emission control system. Modern vehicles have complex emission control systems that include as the primary component a catalytic converter. An electronic engine controller regulates the air-fuel ratio to the engine so that the ratio is as near as possible to the

stoichiometric ratio where the catalytic converter operates most efficiently. During normal operation of the vehicle, the air-fuel ratio is kept at the stoichiometric ratio (lambda = 1). However, there can be cases when the conversion efficiency of the emission control system is reduced. One example is during cold-start events, when the catalytic converter is not at its proper operating temperature and thus is not operating at its peak performance. Another important example includes power enrichment events. When a vehicle has a high engine power demand (which may be induced by a hard acceleration or steep grade), it has been shown that the emission control system can go "open-loop" and the air-fuel ratio is commanded rich for peak demand power and protection of engine components. Recent studies have shown that power enrichment events can contribute significantly to overall emission production (e.g., Meyer et al. 1992; Cadle et al. 1993; Kelly et al. 1993) .

As a first approximation to modeling power enrichment events, a simple thresholding technique is used. When the demanded engine power exceeds a particular threshold, the emission control system goes into an open-loop state, and the air-fuel ratio becomes rich. When the demanded power is below that threshold, the system maintains the air-fuel ratio at stoichiometry.

The emission output of carbon monoxide (CO), hydrocarbons (HC), and oxides of nitrogen (NO_x) can be measured and correlated to demanded engine power induced under numerous operating conditions. The emission output can then be approximated by a function that relates emission species output to demanded power. Such a function may look like figure A1.2. When the demanded engine power is low, the emission control system operates in its regulated state, commanding the air-fuel ratio to stoichiometry. As the demanded power is increased, there is an increased output of emissions since the higher power demand induces greater mass air flow. When the demanded power exceeds a particular threshold, the emission control system commands the air-fuel ratio rich, which results in a significant increase of emissions.

The vehicle dynamics equations and load-based emissions were calibrated to a 1991 Ford Taurus, based on data received from Ford Motor Company. The results of the simulation models with these preliminary data are given in this report. It is important to point out that the emissions for this single vehicle do not represent the emissions behavior for an entire fleet of automobiles. It has been noted that there is large variability in emissions output of different vehicles on identical tests, and even identical vehicles on different tests. Even though the preliminary results in this report are based on a single vehicle, trends can be seen and important conclusions can be made regarding the importance of linking modal emissions with dynamic vehicle activity. As further modal emission data becomes available for other vehicles from Ford and other sources,

they can easily be incorporated into the models when determining a more complete, comprehensive emissions estimate.

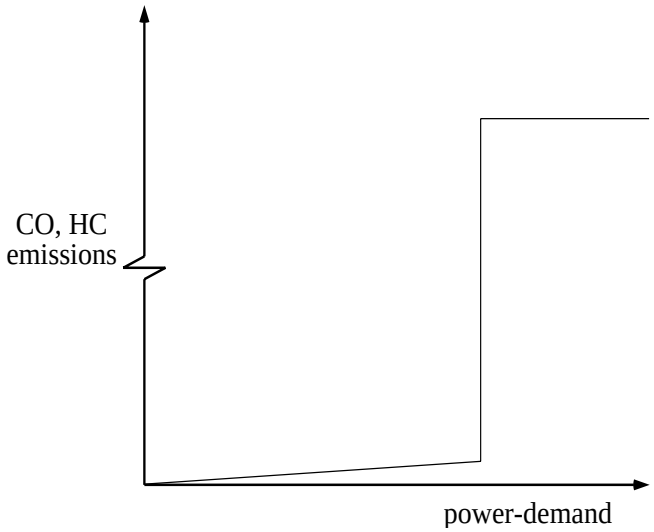

Figure A1.2. CO and HC emissions / power-demand (load) relationship.